

# **Development of a Pilot Scale Membrane Module for Hydrogen Separation**

**Final Report**

**Prepared For**

**New York State Energy Research and Development Authority  
Attn: William Reinhardt  
17 Columbia Circle  
Albany, NY 12203-6399**

**NYSERDA Agreement # 9206-A**

**By**

**Ashok S. Damle  
RTI International  
P. O. Box 12194  
Research Triangle Park, NC 27709-2194**

**October 2008**

## Table of Contents

	<b>Page No.</b>
<b>1.0</b> Summary	1
<b>2.0</b> Background	2
<b>3.0</b> Objectives	3
<b>4.0</b> Task 1 – Bench Scale Testing of Single Short Tubes	4
<b>5.0</b> Task 2 – Scale-up of Composite Membrane Tubes to Longer Lengths	18
<b>6.0</b> Task 3 – Membrane Module Preparation and Testing	21
<b>7.0</b> Task 4 – Technical and Economic Evaluation and Commercialization	31
<b>8.0</b> Conclusions	34
<b>9.0</b> References	35

## List of Figures

	<b>Page No.</b>
<b>Figure 1.</b> Schematic of membrane reactor process with PEM Fuel Cell.	2
<b>Figure 2.</b> SEM cross section of porous media.	6
<b>Figure 3.</b> Composite porous ceramic/stainless steel substrate tube with welded ends.	6
<b>Figure 4.</b> Schematic of membrane test apparatus.	7
<b>Figure 5.</b> Schematic of AccuSep substrate tube with a nonporous stainless steel tube welded on each end.	8
<b>Figure 6.</b> Observed hydrogen permeation rate as a function of temperature and transmembrane hydrogen partial pressure differential for the NPE-3 membrane.	9
<b>Figure 7.</b> Observed hydrogen permeation rate as a function of temperature and transmembrane hydrogen partial pressure differential for the NPE-6 membrane.	9
<b>Figure 8.</b> Observed hydrogen permeation rate as a function of temperature and transmembrane hydrogen partial pressure differential for the PE-2 membrane.	10
<b>Figure 9.</b> Observed hydrogen permeation rate as a function of temperature and transmembrane hydrogen partial pressure differential for the PE-5 membrane.	10
<b>Figure 10.</b> SEM scan of the SS-PE-2 composite membrane tube cross-section.	11
<b>Figure 11.</b> SEM scan of the SS-PE-5 composite membrane tube cross-section.	11
<b>Figure 12.</b> Elemental analysis obtained by EDAX at locations 1 and 2 identified in Figure 11. Composition on the left is at location 1. Composition on the right is at location 2.	12
<b>Figure 13.</b> Observed hydrogen permeation rate as a function of temperature and transmembrane hydrogen partial pressure differential for the PE-052306-1 composite membrane.	14
<b>Figure 14.</b> Observed hydrogen permeation rate as a function of temperature and transmembrane hydrogen partial pressure differential for the NPE-060606-4 composite membrane.	15
<b>Figure 15.</b> Observed hydrogen permeation rate as a function of temperature and hydrogen partial pressure differential for the 82806-6B composite membrane.	16
<b>Figure 16.</b> Observed hydrogen permeation rate as a function of temperature and hydrogen partial pressure differential for the 082806-8B composite membrane over three thermal cycles.	16
<b>Figure 17.</b> Observed hydrogen permeation rate as a function of temperature and hydrogen partial pressure differential for the 032307-2 composite membrane.	17
<b>Figure 18.</b> Photographs of composite membranes with short substrate tubes.	17
<b>Figure 19.</b> Observed hydrogen permeation rate as a function of temperature and hydrogen partial pressure differential for the 111006-1 composite membrane.	18

**List of Figures (contd.)**

	<b>Page No.</b>
<b>Figure 20.</b> Observed hydrogen permeation rate as a function of temperature and hydrogen partial pressure differential over two thermal cycles for the 111006-10 composite membrane.	19
<b>Figure 21.</b> Composite Pd-alloy membrane prepared with 12” active membrane length.	19
<b>Figure 22.</b> Observed hydrogen permeation rate as a function of temperature and hydrogen partial pressure differential for the 12” long 052907-11 composite membrane.	20
<b>Figure 23.</b> Observed hydrogen permeation rate as a function of temperature and hydrogen partial pressure differential for the 12” long 977-Z3 composite membrane element.	21
<b>Figure 24.</b> Schematic of a one-dimensional membrane reactor model.	22
<b>Figure 25:</b> Observed CO conversion in membrane reactor experiments with and without catalyst.	23
<b>Figure 26:</b> Observed CO conversion in membrane reactor experiments without catalyst at 550 °C.	23
<b>Figure 27:</b> Photograph of the pilot-scale test skid. The picture also shows a three-membrane tube module housed inside a 36” long three-zone furnace.	24
<b>Figure 28.</b> Three-tube membrane module held between two rings and Swagelok fittings.	25
<b>Figure 29.</b> Housing shell for multi-tubular module, 2.5” ID, 42” length.	26
<b>Figure 30.</b> Membrane module being loaded in the housing shell.	26
<b>Figure 31.</b> Functional pilot-scale skid with GC and computer control system.	27
<b>Figure 32.</b> Observed CO conversion as a function of net hydrogen recovery at 375 °C.	28
<b>Figure 33.</b> Observed CO conversion as a function of net hydrogen recovery at 550 °C.	28
<b>Figure 34.</b> Hydrogen productivity of the three-tube module.	29
<b>Figure 35.</b> Predicted increase in methane conversion in a membrane reactor.	30
<b>Figure 36.</b> Six-tube membrane module assembled for the methane reforming Demonstration.	30
<b>Figure 37.</b> Six-membrane module connected to the permeate manifold in the bottom flange.	31
<b>Figure 38.</b> Conventional and membrane-reactor-based hydrogen processes.	33

## 1.0 Summary:

This report describes the activities conducted in the project titled, “Development of a Pilot Scale Membrane Module for Hydrogen Separation.” High-performance, high-temperature hydrogen separation membranes represent a key enabling technology for efficient hydrogen production using synthesis gas derived from a variety of feedstocks. In this project, RTI International collaborated with Pall Corporation for developing high flux and selectivity hydrogen separation membranes by depositing thin Pd-alloy films on tubular ceramic/porous stainless steel composite substrates. Both the plating parameters and the inorganic substrate characteristics were modified in an iterative process for producing high hydrogen flux as well as hydrogen selectivity composite membranes. The iterative process involved several progressively improved versions of the Pd-alloy composite membranes. The composite membrane technology was scaled up to produce tubular composite membranes with an active membrane length of 30 cm with membrane surface area of 100 cm<sup>2</sup>. Significant effort was focused on producing reproducible, consistent quality substrate materials as well as composite Pd-alloy membranes.

Developmental Pd-alloy composite membranes were installed in a membrane module consisting of three 12” long membrane elements along with high-temperature water gas shift (WGS) reaction catalyst. WGS reaction was conducted with simultaneous hydrogen separation using the membrane module in membrane reactor configuration for demonstrating production of high-purity hydrogen from simulated synthesis gas. Substantially increased CO conversion was observed in these pilot-scale experiments because of simultaneous hydrogen separation as predicted by model membrane reactor simulations. Greater than 80% of maximum possible hydrogen was recovered in the product stream in membrane reactor operations at temperatures of 375 and 550 °C and pressures of 100 and 150 psig. A membrane module consisting of six 12” long membrane elements was assembled with both methane reforming and WGS catalysts to demonstrate as a functional, pilot-scale hydrogen separation module to produce a high-purity hydrogen product.

## 2.0 Background:

Economical generation of high-purity hydrogen represents a critical technology component for power generation by PEM fuel cells in a variety of mobile and stationary power applications. Hydrogen is commercially produced by steam reforming of hydrocarbon fuels, primarily natural gas, followed by a two-step water gas shift (WGS) reaction and hydrogen separation and purification by pressure swing adsorption (PSA). Hydrogen separation and purification contribute significantly to the capital and operating costs of hydrogen production. Combining the WGS reactor and hydrogen purification steps into a single membrane reactor has the potential to significantly reduce the capital and operating costs of producing hydrogen, especially for small systems, and consequently, reduce the price of hydrogen to the consumer. Due to simultaneous reaction and product separation, it is also possible to increase the efficiency of the overall process by shifting the equilibrium and thereby producing more hydrogen than would be possible using the conventional approach, providing additional benefit to the consumer. The membrane reactor concept can also potentially be used for one-step reforming of natural gas to produce high-purity hydrogen in a compact system. Potential advantages of the membrane reactor-based hydrogen production process include a compact system with a smaller footprint, simpler operation, and lower operating and energy costs. The fuel carbon content is recovered in a compressed, sequestration-ready form. The high purity of the hydrogen product stream allows utilization of efficient power generation technologies, such as PEM fuel cells (Figure 1). The membrane reactor process is especially suited for small-scale “distributed” hydrogen as well as “distributed” power generation.

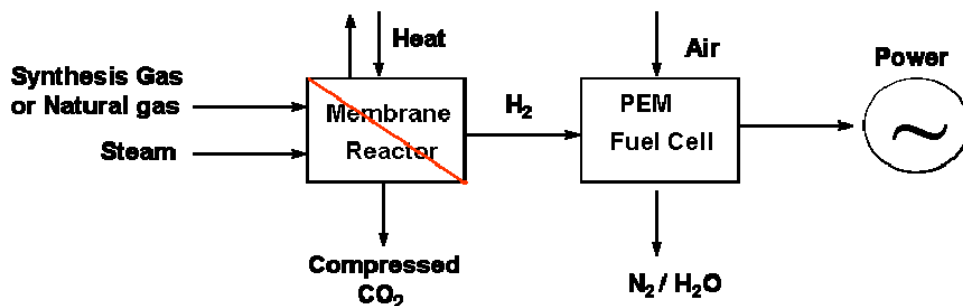


**Figure 1.** Schematic of membrane reactor process with PEM Fuel Cell.

For utilization in high-temperature membrane reactor applications, membranes with high hydrogen permeability and selectivity are needed that are also stable in the WGS and methane reforming process conditions. The candidate membranes for this application include dense ceramic, microporous ceramic, or palladium alloy-based membranes. The dense ceramic membranes based on inorganic perovskite oxides and cermets need high temperatures greater than 700 °C to achieve practical hydrogen flux rates, with fabrication of thin membranes and sealing techniques as key barriers<sup>1,2</sup>. Hydrogen separation based on microporous inorganic membranes provide low hydrogen selectivity (e.g., H<sub>2</sub> to CO<sub>2</sub> selectivity of 3.7)<sup>3</sup>. The selectivity for hydrogen may be increased, at the expense of flux rate, by decreasing the pore size to effect molecular sieving. However, pore size of such membranes is adversely affected by operation in synthesis gas environment, especially due to steam<sup>4</sup>. Palladium-metal-based dense membranes, on the other hand, are completely selective for hydrogen and exhibit an order of magnitude greater hydrogen permeability compared to dense ceramic membranes at considerably lower temperatures of 300-500 °C typical of WGS reaction conditions.

Palladium-alloy foils and extruded tubes are commercially used for small-scale specialized hydrogen purification systems; however, they are a relatively expensive option for large-scale industrial hydrogen production. These product formats exhibit low hydrogen flux rates due to the thickness necessary for structural stability. By depositing thin palladium-alloy film on a suitable porous substrate, hydrogen flux and structural stability of the composite Pd-alloy membrane may be increased while reducing the membrane costs. Electroless plating process has been successfully used in a number of studies to prepare Pd-composite membranes<sup>5,6,7</sup>. While the hydrogen flux rate through a Pd-alloy composite membrane primarily depends on the membrane thickness, temperature, hydrogen partial pressure differential (Sievert's law), and alloy composition; the substrate pore size and surface characteristics are highly influential for the mechanical and thermal stability of the composite membranes<sup>8</sup>. The challenge in synthesizing composite membranes is to produce thin yet defect-free and stable alloy films on the substrate (as even small pinholes would be detrimental to the hydrogen selectivity) and to reduce overall cost.

The U.S. Department of Energy (DOE) has set performance and cost targets<sup>9</sup> for developing Pd-alloy composite membranes. The year 2010 DOE targets include hydrogen flux target of 250 scfh/ft<sup>2</sup> and membrane module cost target of \$1,000/ft<sup>2</sup>. Combining these two targets into a single goal of \$4/scfh of hydrogen capacity sets a relevant, challenging goal for commercialization of the Pd-alloy composite membranes. The overall goal of this project effort was to develop low-cost Pd-alloy composite membranes with high hydrogen flux and selectivity properties as well as manufacturability for producing consistent, reproducible, quality membranes and demonstrate their application for hydrogen production applications.

### **3.0 Objectives:**

The objective of this cost-shared research effort by Research Triangle Institute (RTI) and Pall Corporation was to advance Pd-alloy-based hydrogen separation membrane technology to a pilot-scale unit meeting the cost and performance targets identified by U.S. DOE for dense metallic membranes. The research effort was conducted in four tasks:

Task 1 – Bench Scale Testing of Single Short Tubes - The objective of this task was to develop short tubular membrane elements of optimum palladium alloy/substrate composite membrane configuration and composition to be able to meet or exceed the membrane performance and cost targets. In this task, a number of short composite membranes (2" to 8" long) were prepared to determine the effect of substrate material and pore size distribution, substrate surface characteristics, membrane deposition and annealing procedures, membrane thickness, and alloy composition for preparing thin, low-cost, yet robust and durable Pd-alloy composite membranes. Several generations of substrate and composite membranes were prepared in this task as improvements to the substrates were made over the course of this task by Pall Corporation.

Task 2 – Scale-up of Composite Membrane Tubes to Longer Lengths - The objective of this task was to focus on scale-up of the composite membranes to commercial-size tubular elements by developing procedures to synthesize reproducibly long, tubular Pd-alloy composite membrane elements of desired specifications. Substrate and composite membrane synthesis procedures were

scaled up in this task to 12” long membrane elements with a focus on membrane uniformity and mass production ability to minimize manufacturing costs.

Task 3 – Membrane Module Preparation and Testing – The objective of this task was to prepare a functional, pilot-scale membrane module capable of producing and separating a target 7 kg/day of hydrogen (~54 std. liters/min) using membrane elements prepared with optimized synthesis parameters and specifications. A multi-tubular, pilot-scale module capable of separating 50 liters/min of hydrogen was fabricated and tested in this task.

Task 4 – Technical and Economic Evaluation and Commercialization – The objective of this task was to conduct technical and economic assessment of the Pd-membrane-based hydrogen production technology. Potential reduction in cost of hydrogen production by utilization of Pd-membrane reactor technology was assessed by using U.S. DOE’s H2A hydrogen cost model.

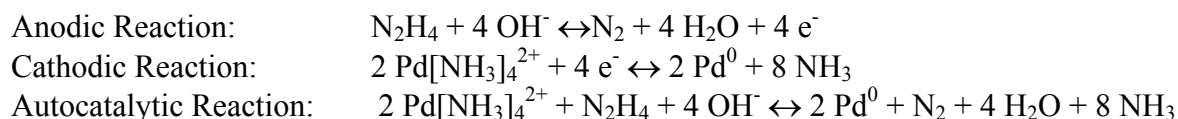
#### **4.0 Task 1 - Bench Scale Testing of Single Short Tubes**

Both the thin metal film deposition process and the porous substrate characteristics influence successful development of composite membranes for hydrogen separation application. Porous ceramic as well as porous stainless steel supports have been used for preparation of Pd-alloy composite membranes with electroless plating technique<sup>5,6,7</sup>. Electroless plating process is molecular in nature and occurs over the entire activated porous surface. A dense continuous film will be formed on a porous substrate surface only after plugging all the pore openings on the surface. The size and distribution of pore openings on the substrate surface thus determine the minimum thickness required to form a leak-tight film. Porous ceramic supports typically consist of graded structure with fine pore size layers deposited on a much coarser support. The top fine pore size layer is formed by depositing colloidal ceramic particles with a uniform homogeneous layer with pore size in the range of 1 to 200 nm depending upon specific ceramic material used<sup>10</sup>. Although ceramic supports provide excellent surface characteristics for depositing thin palladium alloy films, ceramic materials are brittle and require special ceramic to metal seals for use in high temperature environment. Porous metal supports on the other hand offer advantages of mechanical strength, ease of handling, and welded end connections, however, they are much coarser compared to ceramic supports and require much thicker plating for producing leak-tight films with high selectivity.

In this project, RTI collaborated with Pall Corporation for developing Pd-alloy composite membranes using porous ceramic/metal composite substrate media combining the best features of both porous ceramic and porous metal substrates. These inorganic substrates consist of a ceramic membrane layer (nominal 0.1- $\mu\text{m}$ -grade zirconia) embedded on the surface of a coarser ~2- $\mu\text{m}$ -grade porous stainless steel support tube (AccuSep<sup>®</sup> Inorganic media.) Nonporous stainless steel tubing may be welded to the ends of the porous metal tube for easy assembly and sealing in the membrane modules. Electroless plating process was used in this effort to deposit metal films on the surface of the ceramic layer with subsequent thermal annealing in an inert atmosphere to form Pd-alloy composite membranes. In RTI’s patented electroless plating technique<sup>11</sup>, the liquid plating solutions are continuously circulated over the porous substrate surface. The penetration of the plating solution in the porous structure of the substrate is controlled by maintaining an appropriate opposing inert gas pressure. The result is uniform deposition of metal on the substrate with adequate

anchoring in the porous network for excellent adhesion and mechanical membrane stability. This technique is amenable to scale-up to long tubes and automation.

Electroless plating is a well-studied, three-step process involving pretreatment of the substrate, sensitization and activation of the substrate surface, and electroless plating, which is a combination of cathodic deposition of metal and anodic decomposition of reductant. Palladium deposition occurs as the result of the following simultaneous reactions:



Each of the three steps is critical for uniform deposition of the palladium metal film. The sensitization and activation process, involving adsorption of  $\text{Sn}^{2+}$  ions on the substrate followed by substitution by Pd, produces finely divided palladium metal nuclei on the substrate that initiate the autocatalytic plating process. The  $\text{PdCl}_2$  may be replaced by  $\text{AgNO}_3$  solution for silver metal plating. Somewhat different but also well-known electrochemistry<sup>6</sup> is used for deposition of copper metal for preparing Pd-Cu alloys.

Pure palladium metal becomes brittle and is prone to distortions during thermal cycling due to the dimensional changes caused by transformations between the  $\alpha$ -phase palladium, which is stable at low temperatures, and the  $\beta$ -phase palladium, which is stable at high temperatures. Alloying elements such as Ag stabilizes the  $\beta$ -phase against the  $\alpha$ -phase, substantially reducing metal embrittlement. Pd-Ag alloy also exhibits greater permeability for hydrogen than pure palladium at similar conditions. An alloy with 23% Ag and 77% Pd has been shown to have the maximum permeability as well as dimensional stability<sup>12, 13</sup>. Pd-Ag alloys also have significantly higher permeability for hydrogen than Pd-Cu alloys and were therefore used in this composite membrane development effort, which, in large part, was dictated by the ongoing substrate development need. A Pd-to-Ag ratio of 3:1 was targeted in sequencing the metal platings.

The performance and cost of Pd-alloy composite membrane strongly depend on the quality of both substrate and Pd-alloy layer deposition technique. More uniform, finer pore size of the porous support will lead to a thinner Pd-alloy membrane. In case of the ceramic/metal composite substrates, the deposition and adhesion of the ceramic (zirconia) layer on the porous stainless steel is also important in addition to adhesion of Pd-alloy layer to the ceramic top-layer. The Pd-alloy composite membranes were therefore developed through interactive improvement of both porous substrate characteristics and plating parameters to obtain defect-free, high hydrogen flux and selectivity, low-cost Pd-alloy composite membranes. Yttria-stabilized zirconia (YSZ) is preferred for the ceramic membrane layer because its thermal expansion coefficient is similar to that of the palladium metal. The YSZ membrane layer consists of an average pore diameter of ~70 nm. The base metallic porous

support tube is made of porous stainless steel with a nominal  $\sim 2 \mu\text{m}$  average pore size capable of operation at  $550^\circ\text{C}$  and 20 bar (300 psig) transmembrane pressure differential ( $\Delta P$ ). Figure 2 shows SEM scan of the cross-section of the composite porous ceramic/metal media, and Figure 3 shows a substrate tube with nonporous SS tube welded ends and YSZ coating on the outside area of tube.

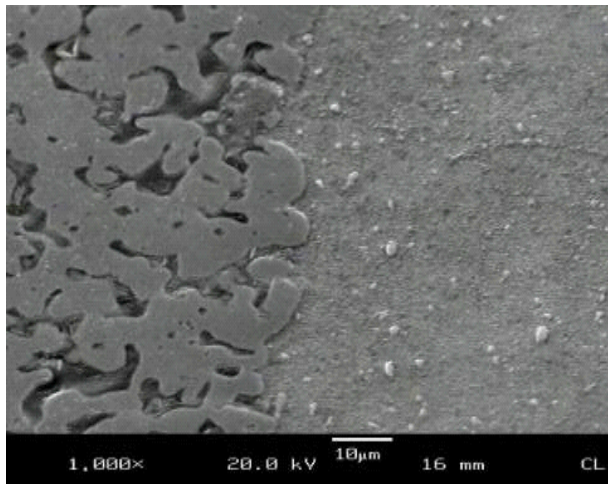


**Figure 2.** SEM cross-section of porous media.

Several generations of substrate materials in short tubes were prepared and evaluated for defect-free Pd-alloy composite membrane preparation and testing in this project in a much larger part of this program than originally anticipated. The results obtained with these versions are described below. Substrate variations included procedures for depositing zirconia layer, integrity and thickness of the zirconia layer, material and grade of stainless steel used for porous support tube, welding of non-porous ends, and surface treatment/smoothing. Composite Pd-alloy membranes were prepared by depositing individual metals by electroless plating as described above followed by thermal annealing. The plating time and amount was essentially determined by the substrate characteristics to form a smooth non-porous dense film on the bulk of the substrate surface. The non-uniformities in zirconia coating and the upper size range in the pore size distribution often resulted in pin-hole defects where essentially most of the surface appeared to be non-porous.

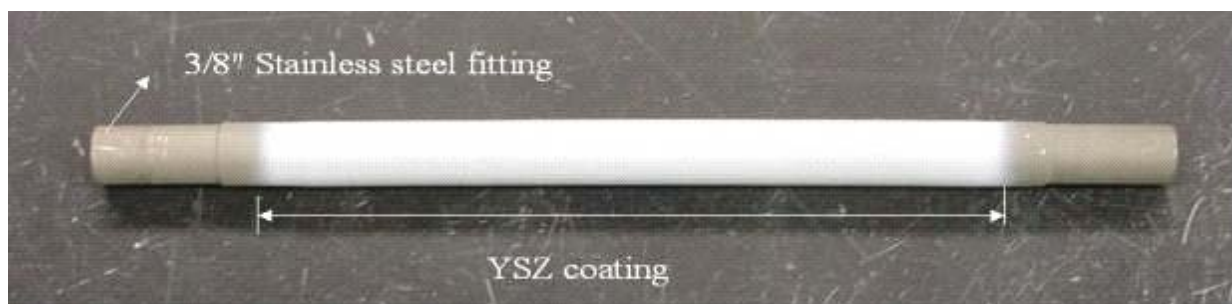


**Figure 3.** Composite porous ceramic/stainless steel substrate tube with welded ends.

Pure component as well as mixed gas permeation characteristics of the developmental Pd-alloy composite membranes were measured at membrane temperatures in the range of  $300$  to  $600^\circ\text{C}$  and up to 40 psi transmembrane hydrogen partial pressure differential using the experimental test apparatus shown schematically in Figure 4. No sweep gas was used in these measurements with nearly pure hydrogen on the permeate side at atmospheric pressure. The hydrogen and nitrogen flux rates were determined by appropriate size bubble flow meters. A 24" long tubular bench-top furnace was used for testing both the short and scaled-up, 12" long, composite membrane elements.

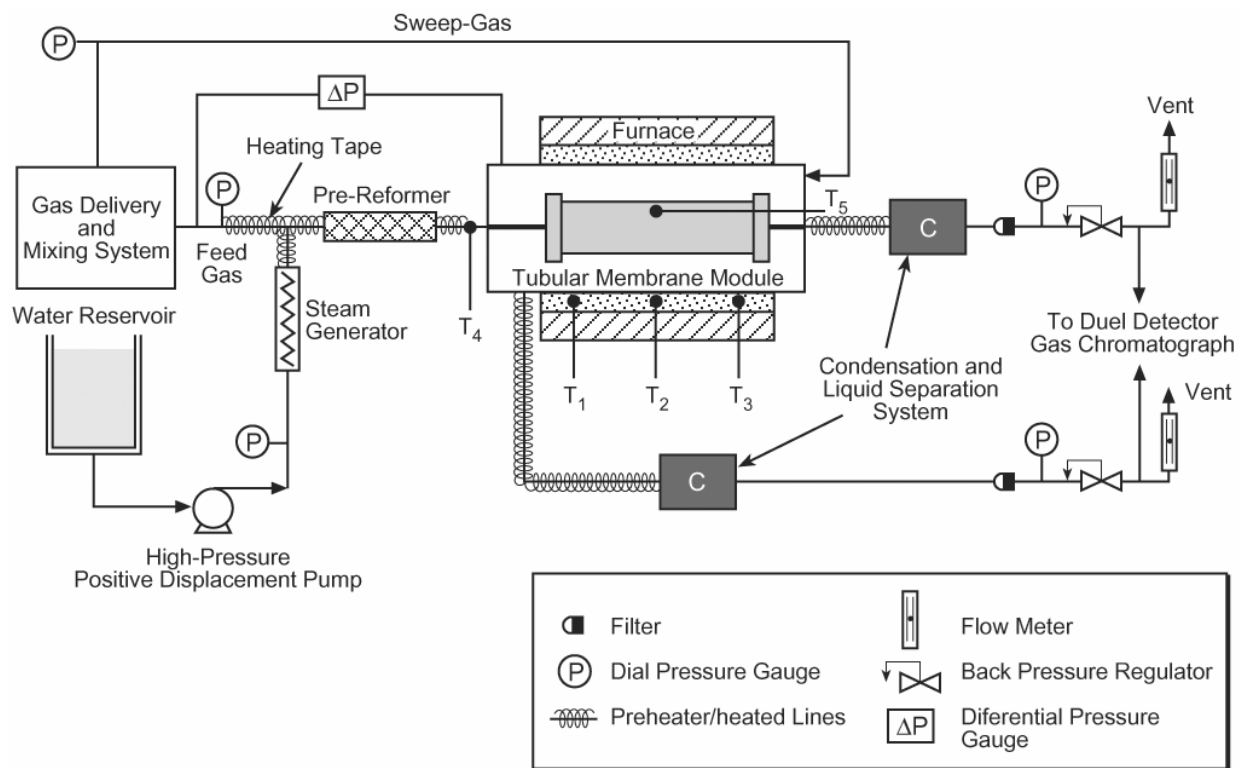


**Figure 4.** Schematic of membrane test apparatus.

Substrate Version 1 - SS-NPE series – This series of tubes were approximately 0.41” in diameter and consisted of 7” long porous media with non-porous ¼” OD stainless steel tubes welded to both ends as shown in Figure 5. The porous stainless steel section of these tubes was covered on the outside surface of the tubes by a zirconia layer with a nominal pore size of 0.1 micron. High hydrogen flux rates were observed for Pd-alloy composite membranes prepared with this series of tubes as shown in Figure 6 for NPE-3 (non porous end connection type) composite membrane. The observed hydrogen to nitrogen pure component selectivity at 500 °C was of the order of 500 to 1,000. The NPE-3 composite membrane tube was subjected to five (5) thermal cycles (25 °C to 600 °C) over a 25-day period to determine the effect of thermal cycling on the membrane performance. The hydrogen flux rate characteristics remained the same over the thermal cycles. The pure component hydrogen to nitrogen selectivity however decreased from about 1,250 during the first thermal cycle to about 500 by the third thermal cycle remaining constant thereafter for the next two thermal cycles. The membrane performance of the NPE-3 was also confirmed with mixed gas permeation tests with H<sub>2</sub>:N<sub>2</sub>::50:50 mixed gas feed. Similar high flux observed with NPE-6 membrane is shown in Figure 7 which exhibited slightly greater pure component hydrogen to nitrogen selectivity of 2,080 at 600 °C and 40 psi pressure differential.

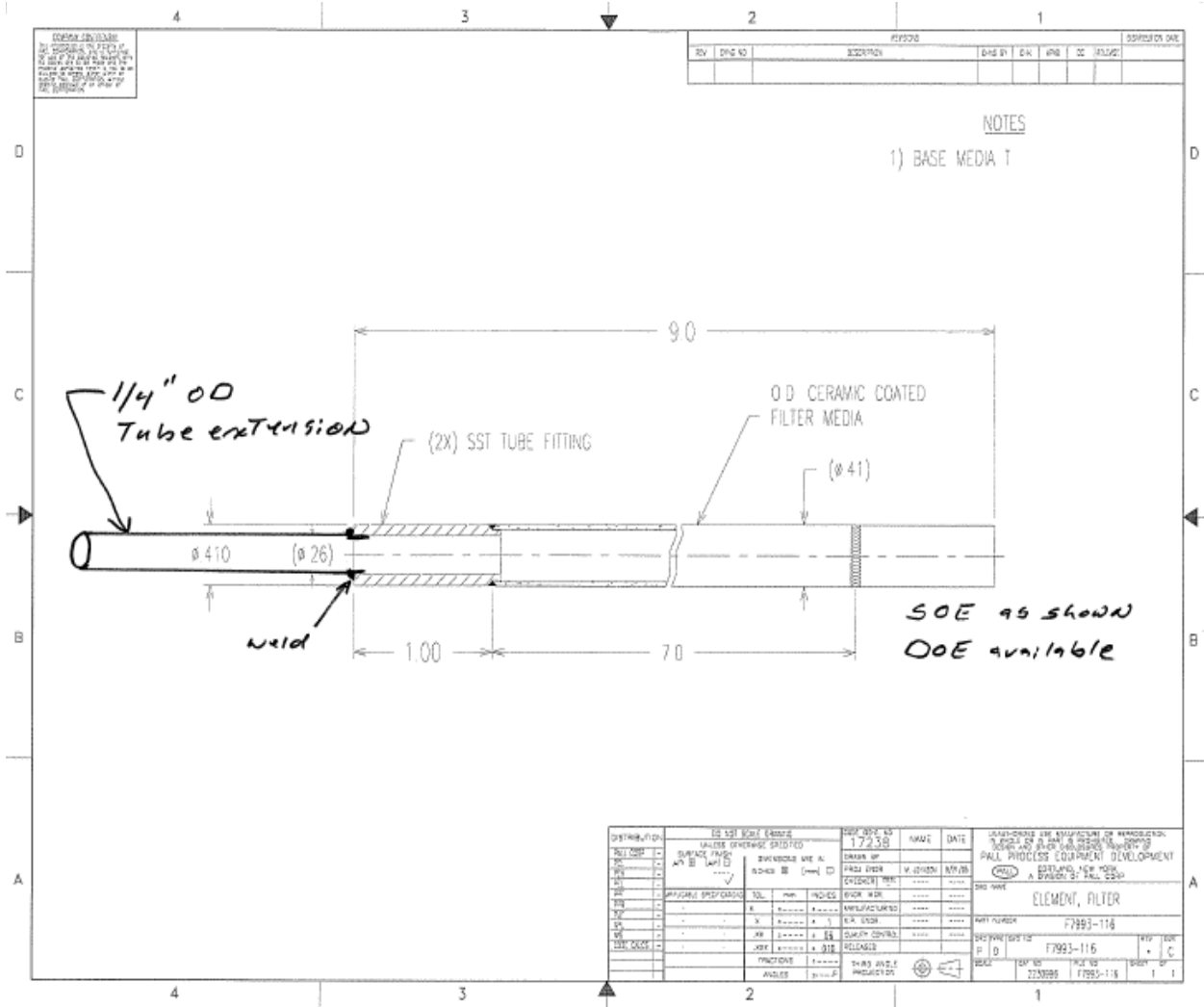


**Figure 5.** Schematic of AccuSep substrate tube with a nonporous stainless steel tube welded on each end.

Substrate Version 2 – SS-PE series - This set of tubes consisted of approximately 8” long porous media section, 0.46” in diameter tapered to 10 mm OD to allow use of standard 10 mm Swagelok fittings. No non porous tubes were welded to these tubes. Observed hydrogen permeation characteristics for PE-2 composite membrane are shown in Figure 8 and that for PE-5 is shown in Figure 9. A number of samples of the composite membrane tube sections were sent to Pall Corporation for metallographic sectioning and detailed SEM and EDAX elemental analysis of the composite membrane. The SEM analysis has been useful to determine the nature and possible cause of any defects e.g. peeling of ceramic layer as observed earlier. Such analysis is also useful to determine the Pd-alloy film thickness, homogeneity of the metal layer and penetration of the metal in the zirconia layer which is essential for thermal and mechanical stability of the film. Figure 10 shows the SEM scan of the cross section of the PE-2 composite membrane indicating a uniform homogeneous dense film of Pd-alloy membrane of about 3.5 µm. Figure 11 shows close-up scan of PE-5 composite membrane again indicating a dense metal film of about 3.5 µm average thickness. The SEM scan also clearly shows the anchoring of the film in the ceramic layer about 4 µm deep.

The elemental analysis conducted within the dense film and within the top portion of the ceramic layer clearly indicates (Figure 12) the penetration of the Pd-alloy in the ceramic layer essential for thermal and mechanical stability of the composite membrane.

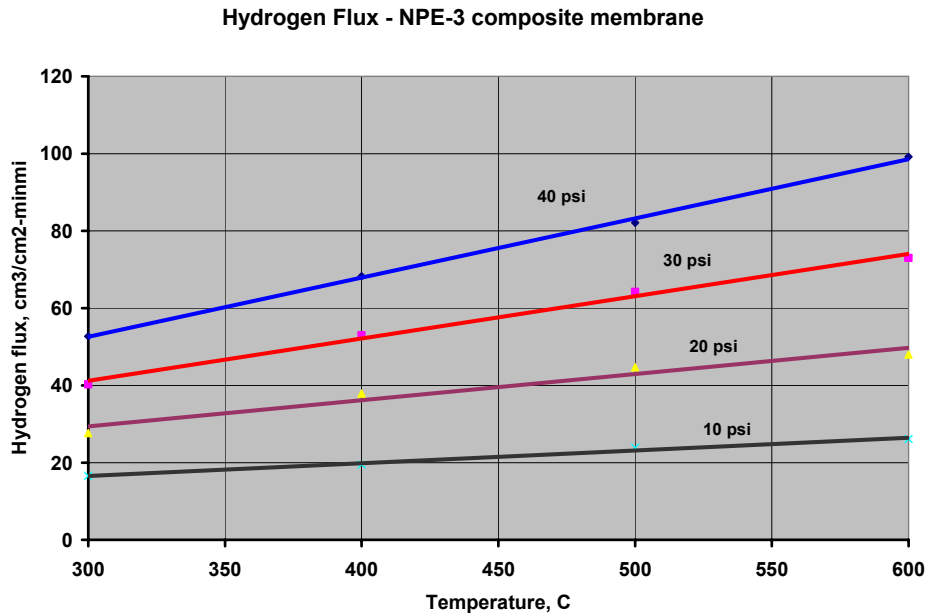


**Figure 6.** Observed hydrogen permeation rate as a function of temperature and transmembrane hydrogen partial pressure differential for the NPE-3 membrane.

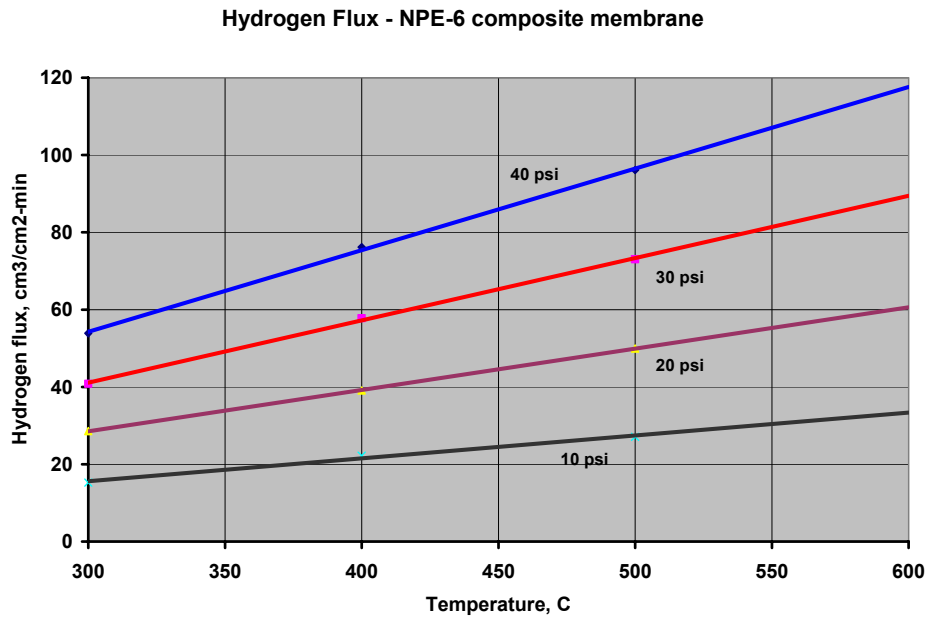


**Figure 7.** Observed hydrogen permeation rate as a function of temperature and transmembrane hydrogen partial pressure differential for the NPE-6 composite membrane.

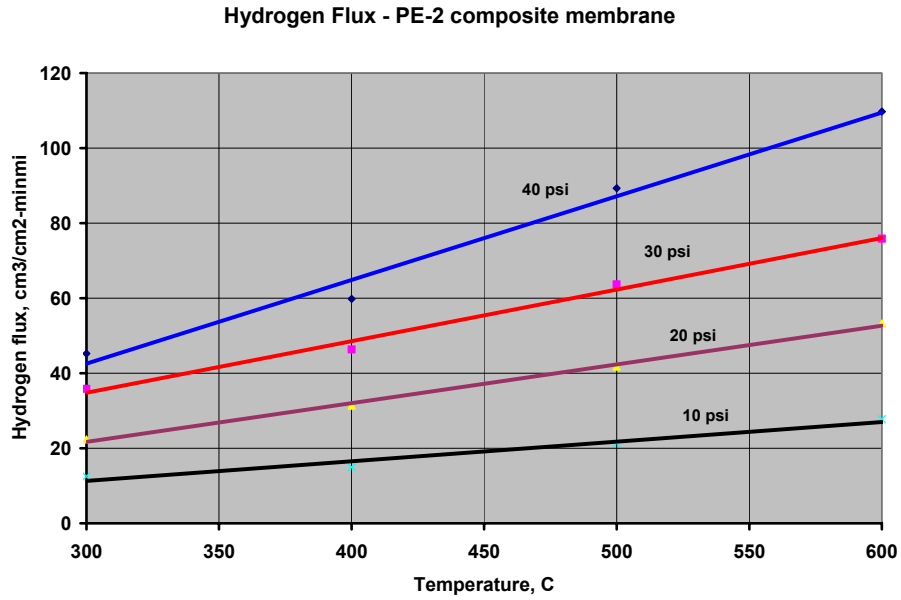


**Figure 8.** Observed hydrogen permeation rate as a function of temperature and transmembrane hydrogen partial pressure differential for the PE-2 membrane.

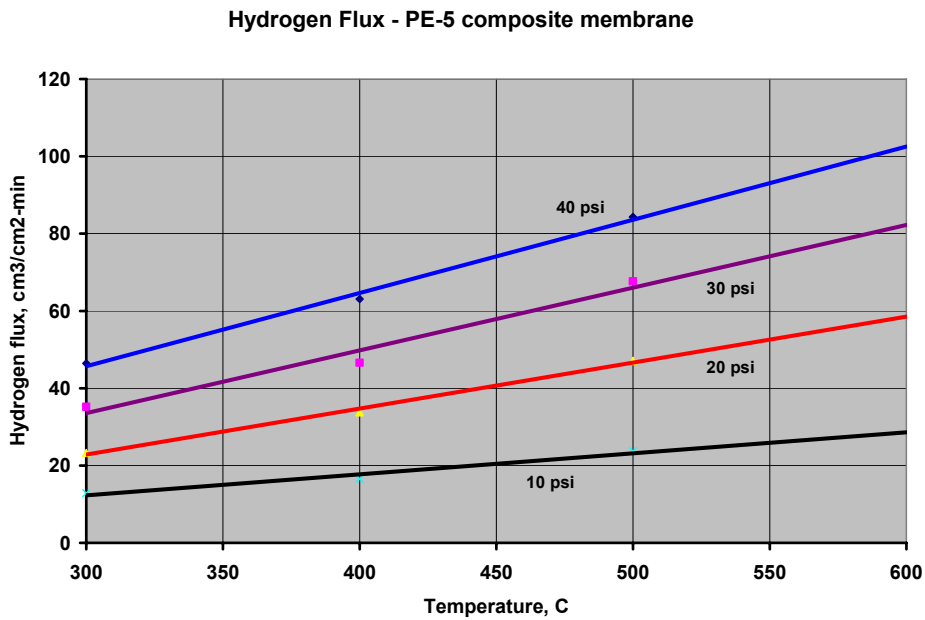


**Figure 9.** Observed hydrogen permeation rate as a function of temperature and transmembrane hydrogen partial pressure differential for the PE-5 membrane.

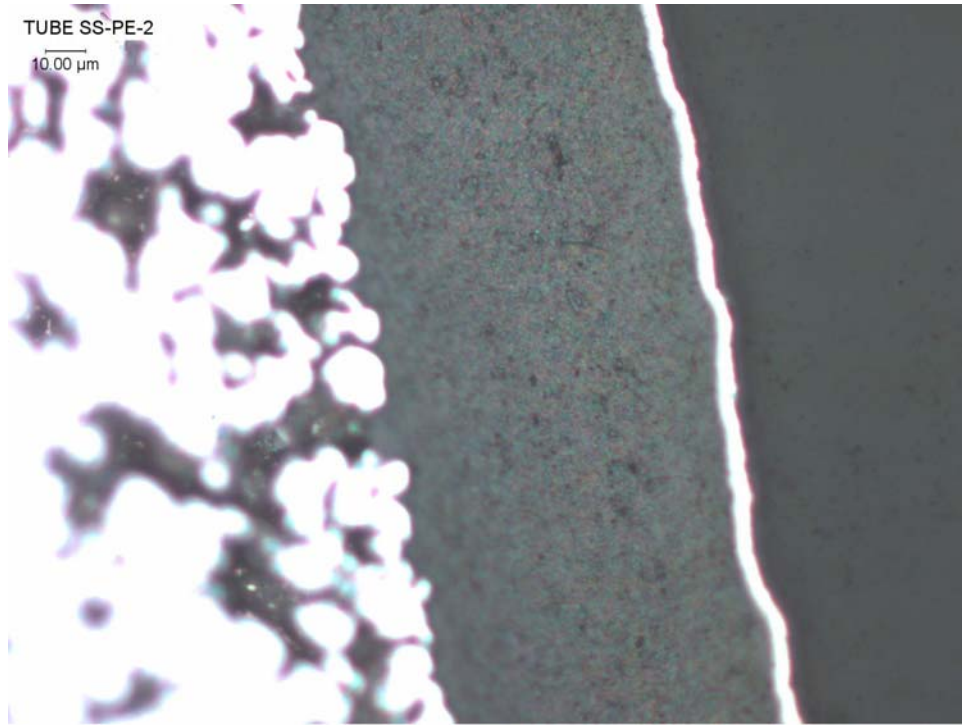


**Figure 10.** SEM scan of the SS-PE-2 composite membrane tube cross-section.

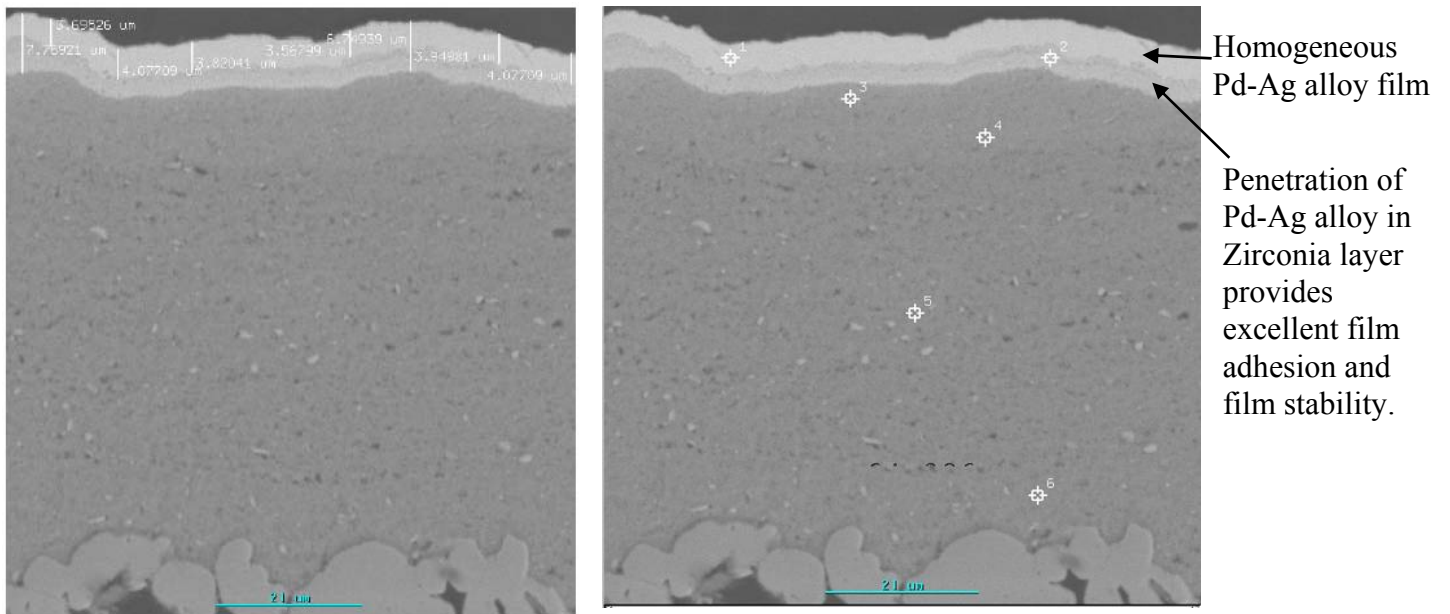


**Figure 11.** SEM scan of the SS-PE-5 composite membrane tube cross-section.

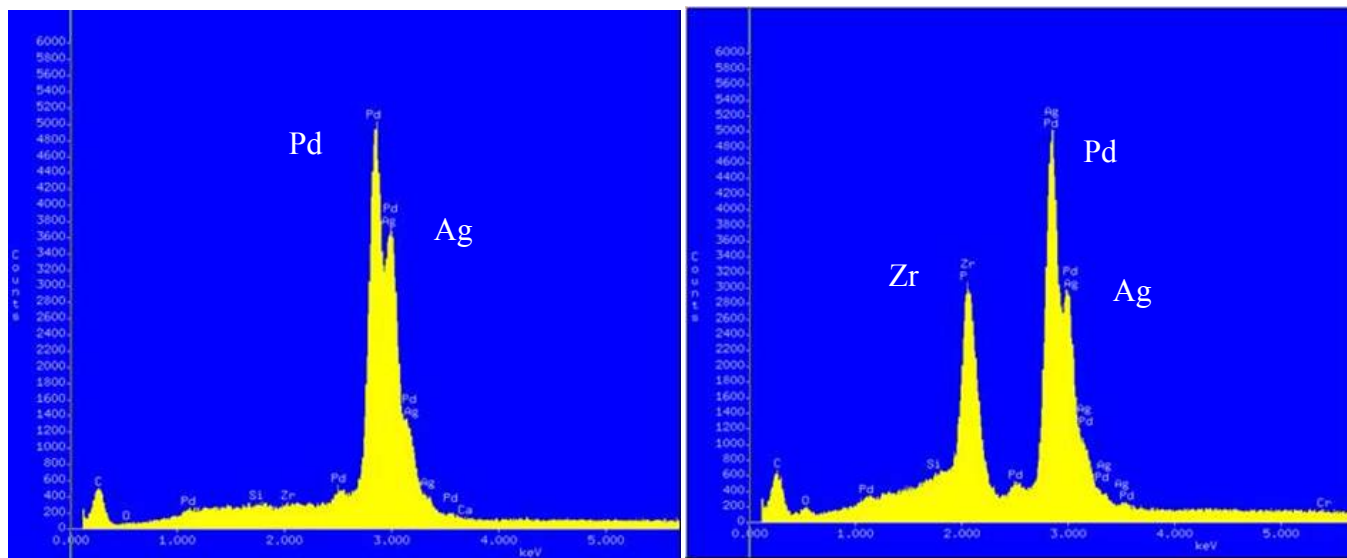


**Figure 12.** Elemental analysis obtained by EDAX at locations 1 and 2 identified in Figure 11. Composition on the left is at location 1. Composition on the right is at location 2.

The support material for NPE tubes was made from 316L porous stainless steel (SS) having a 0.8 micron average pore diameter, whereas, the support material for PE tubes was made from 316L porous stainless steel (SS) having a 2.0 micron average pore diameter. The porous stainless steel sections of all tubes were covered on the outside surface of the tubes by a zirconia layer with a nominal pore size of 0.1 micron. Due to the finer pore size, the integrity of zirconia coating was determined to be better for the NPE tubes as measured by fluid (Pallsol – Pall Corporation’s proprietary test liquid) flux rate through the support tubes at a constant fluid pressure differential.

While successful composite membranes were prepared with these substrate materials as indicated by the above described performances, the sensitivity of the porous stainless steel to the aqueous solutions was also noted causing detachment of the ceramic layer from the porous stainless steel at isolated spots in some of the membrane preparations. Two tubes in each set of the tubes could not be tested for permeation due to isolated peeling areas on the tube surfaces. The problem was traced to residual ionic solutions left in the porous stainless steel matrix after rinsing the tubes in DI water. Discussions with Pall Corporation confirmed the sensitivity of porous stainless steel to ionic aqueous solutions involved in the aqueous-phase electroless plating process. Thorough rinsing of the membrane tubes with deionized water, including using warm water, after every processing step was considered to be the primary remedy and was used in subsequent membrane preparations.

Although the composite membranes prepared with the tubes of the two distinct support designs indicated similar hydrogen flux rates the observed pure component hydrogen to nitrogen selectivity was decidedly much greater with NPE type tubes as compared with PE type support tubes. For example, the hydrogen permeation rates shown in Figures 7 and 9 for NPE-6 and PE-5 composite membranes were similar, however, the pure component hydrogen to nitrogen selectivity for NPE-6 membrane at 600 °C and 40 psi pressure differential was about 2,080 and that for PE-5 composite membrane was about 285 for the same permeation test conditions. The smaller pore size in the porous stainless steel and the improved zirconia coating integrity in NPE tubes are the likely reasons

for the observed greater selectivity of the composite membranes prepared with NPE type tube supports.

In addition to the underlying porous stainless steel pore size and porosity, the smoothness of the surface of the ceramic zirconia layer is also expected to have an influence on the palladium membrane coating process and the performance of the composite membrane. Pall Corporation developed a process to prepare zirconia layers with different surface smoothness as measured in micro-inches by a Taylor-Hobson, Talysurf profilometer. Two batches of six substrate tubes each was prepared by Pall Corporation with similar stainless steel porous material as in the NPE tubes but with smoother surface with surface roughness in the range of 35 to 45 micro-inches described below.

Substrate Version 3 – 052306 series and Substrate Version 4 – 060606 series - The two sets of AccuSep substrate tubes (052306 and 060606 series) consisted of six (6) tubes each of two different designs with modifications to the earlier PE and NPE version designs. Both sets of tubes used 316L porous stainless steel base tube material with a nominal pore rating of 1  $\mu\text{m}$  and were approximately 0.41” in diameter. The 052306 series tubes were about 5.25” in length and were coated by a 25-30  $\mu\text{m}$  thick zirconia layer of a nominal pore size of 0.1  $\mu\text{m}$  with a proprietary coating method “A”. All tubes in this series received a proprietary surface modification step intended to reduce the surface roughness to allow for formation of thinner membranes. The 060606 series of tubes consisted of 3/8” OD and 1” long, nonporous 316 L stainless steel tube sections welded to each end of the porous stainless steel base tube. The overall length of the tubes in this series was 9” with a porous section of 7”. Five tubes in this series were coated by a 25-30  $\mu\text{m}$  thick zirconia layer of a nominal pore size of 0.1  $\mu\text{m}$  with a proprietary coating method “A” and received a proprietary surface modification step intended to reduce the surface roughness to allow for formation of thinner membranes. One tube in this 060606 series used another proprietary coating method “B” to deposit a 10-15  $\mu\text{m}$  thick zirconia coating. No additional surface modifications steps were undertaken to change the surface roughness for this method “B” tube.

Pd-alloy composite membranes were prepared using four substrate tubes from each of the 052306 and 060606 series. Due to sensitivity of the porous stainless steel to ionic aqueous solutions involved in the aqueous-phase electroless plating process, thorough rinsing of the membrane tubes with deionized water was used after each processing step (e.g., activation and each metal plating sequence). The rinsate solution was monitored by water conductivity measurements to assure removal of ionic species from the porous stainless steel structure. In spite of the thorough cleaning procedures used, the peeling of the ceramic zirconia layer at a few isolated spots persisted with the 052306 series of substrate tubes and the first of the 060606 series of the tubes evaluated. The composite membranes prepared with the 052306 series of substrate tubes, however, indicated high hydrogen flux rates. Because of the high hydrogen flux rates, the hydrogen to nitrogen selectivity was still reasonably high. The observed hydrogen flux rate of a composite membrane prepared with PE-052306-1 substrate tube is shown in Figure 13. The hydrogen to nitrogen selectivity at 600 °C for this membrane was about 2,000.

Preparation of composite membranes with the 060606 series substrate tubes, in general, needed greater amount of plating to form a leak-tight membrane film. Except for the first substrate tube evaluated from this series, three of the composite membranes did not indicate any peeling of the ceramic layer from the porous stainless steel surface. These three composite membranes also

indicated remarkable hydrogen to nitrogen selectivity in the permeation evaluations, with two of the membranes tested indicating no measurable nitrogen permeation over three thermal cycles (25 °C – 600 °C – 25 °C) with absolute hydrogen selectivity. The observed hydrogen flux rate with one of the membranes in this series, NPE-060606-4, is shown in Figure 14. Because of the greater amount of metal plated that increased the corresponding film thickness for this membrane, the hydrogen flux rate observed with this composite membrane is somewhat lower than that observed for PE-052306-1, however, with a tradeoff for greater hydrogen selectivity.

Hydrogen Flux - PE-052306-1 composite membrane

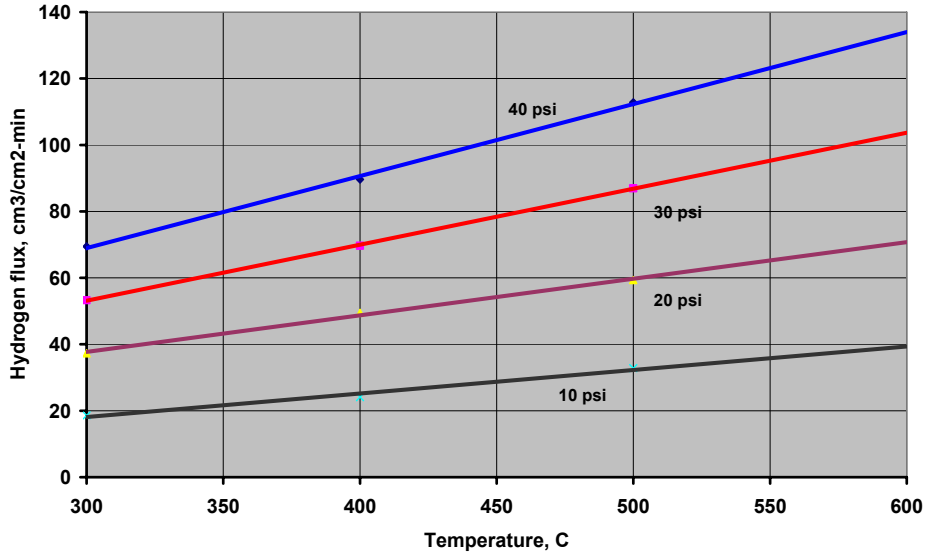


**Figure 13.** Observed hydrogen permeation rate as a function of temperature and transmembrane hydrogen partial pressure differential for the PE-052306-1 composite membrane.

Substrate Version 5 – 082806 series - This set of five (5) tubes used 316L porous stainless steel base tube material with a nominal pore rating of 1 μm with a void volume of 23% and were approximately 0.41” in diameter. These tubes consisted of 3/8” OD and 1” long nonporous 316 L stainless steel tube sections welded to each end of the porous stainless steel base tube. The overall length of the tubes in this series was 6.1” with a porous section of 3.75”. Based on the results of the Pd-alloy composite membranes prepared with the earlier sets of AccuSep substrate tubes (052306 and 060606 series) the Zirconia layer was applied by using variations of type “B” coating technique dropping the Zirconia coating style “A” completely. The zirconia coating thickness in these tubes was about 20 to 30 μm thick. There were three versions of coating style “B” utilized, B, B1, and B2. The difference being the level of integrity achieved, with B2 the best integrity, B1 next, and B the lowest. The permeability of each style was reduced as the integrity was improved. The purpose of these changes was to help determine which level of integrity was needed to provide a good Pd coating. The substrate tubes are characterized by the surface roughness as well as by a measure of integrity as determined by the permeation of a proprietary material “Pallsol” at 40 psig differential.

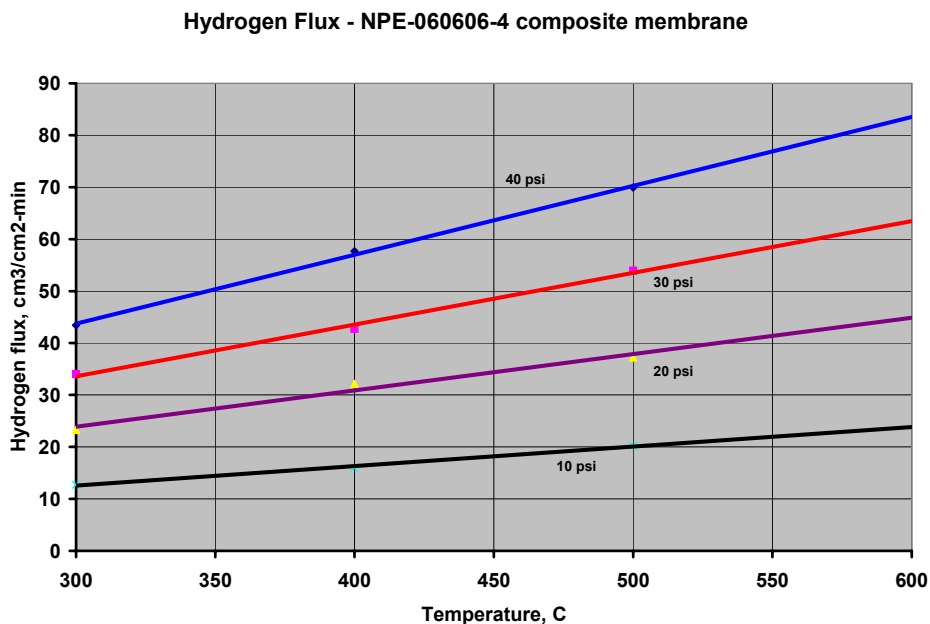


**Figure 14.** Observed hydrogen permeation rate as a function of temperature and transmembrane hydrogen partial pressure differential for the NPE-060606-4 composite membrane.

Pd-alloy composite membranes were prepared using all five of the substrate tubes from the 082806 series. Due to sensitivity of the porous stainless steel to ionic aqueous solutions involved in the aqueous-phase electroless plating process, thorough rinsing of the membrane tubes with deionized water was used after each processing step (e.g., activation and each metal plating sequence). The rinsate solution was monitored by water conductivity measurements to assure removal of ionic species from the porous stainless steel structure. No peeling of the ceramic zirconia layer was observed during palladium plating of these tubes indicating improved zirconia coating as well as the welding technique used for attaching non porous sections to these tubes. The hydrogen permeation results obtained with a composite membrane 082806-6B is shown in Figure 15 with performance similar to that observed for earlier membranes. The observed hydrogen to nitrogen pure component selectivity for this composite membrane was ~400 at 600 °C. A slightly thicker Pd-alloy film membrane was prepared next resulting in a defect-free composite membrane 082806-8B. This membrane was exposed to three thermal cycles of 25-600-25 °C over a two-week period, indicating reproducible hydrogen permeation rates and no nitrogen leak at 40 psig pressure. The high hydrogen selectivity was also confirmed in the mixed gas permeation tests conducted using 50% H<sub>2</sub>-50% N<sub>2</sub> gas mixture. The permeate hydrogen purity was about 99.93% with a mixed gas H<sub>2</sub>:N<sub>2</sub> selectivity of 1,600. The hydrogen permeation data obtained over the three thermal cycles is shown in Figure 16.

Substrate Version 6 – 032307 series - Based on the results obtained with short tubes in the five earlier versions, reproducibility of the substrate production process was verified by Pall Corporation by producing a number of short 2” long tubes with welded non-porous end tubes. A batch of ten (10) tubes of series 032307 was received by RTI to verify reproducibility of the plating technique. Pd-Ag alloy composite membranes were prepared using these substrates and tested for their permeation characteristics. A somewhat improved hydrogen performance was observed with the

composite membranes prepared with the new batch of substrates than that obtained with the earlier versions of the substrate tubes. Results obtained with a composite membrane 032307-2 are shown in Figure 17. The observed pure component selectivity for H<sub>2</sub> permeation for this membrane was about 3,500 compared to nitrogen at 300-600 °C membrane temperature.

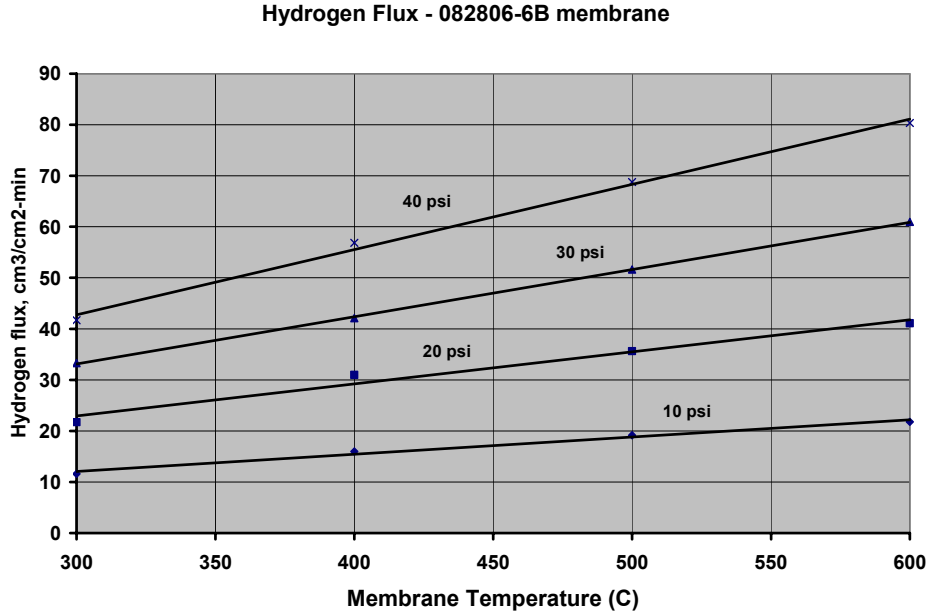


**Figure 15.** Observed hydrogen permeation rate as a function of temperature and hydrogen partial pressure differential for the 82806-6B composite membrane.

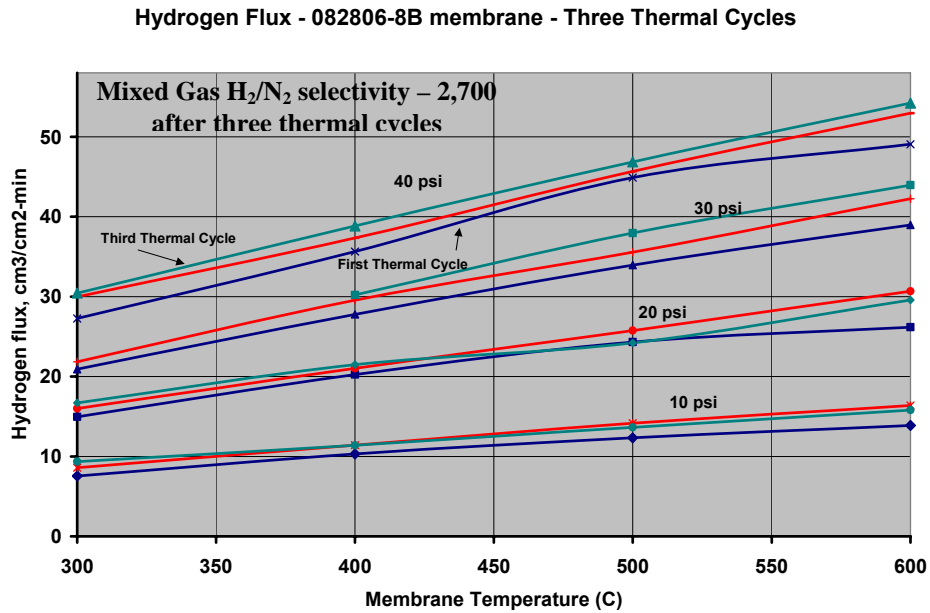


**Figure 16.** Observed hydrogen permeation rate as a function of temperature and hydrogen partial pressure differential for the 082806-8B composite membrane over three thermal cycles.

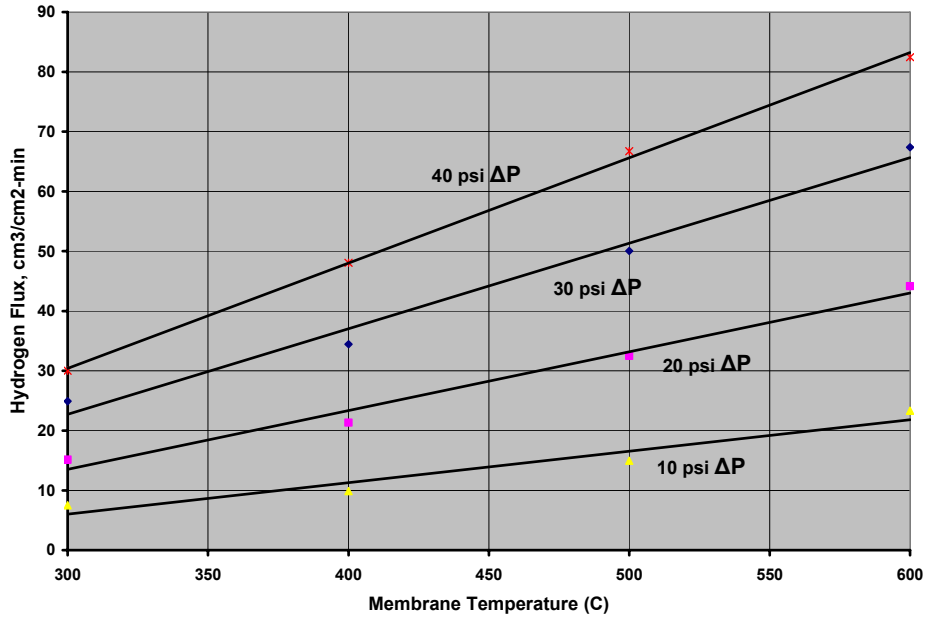
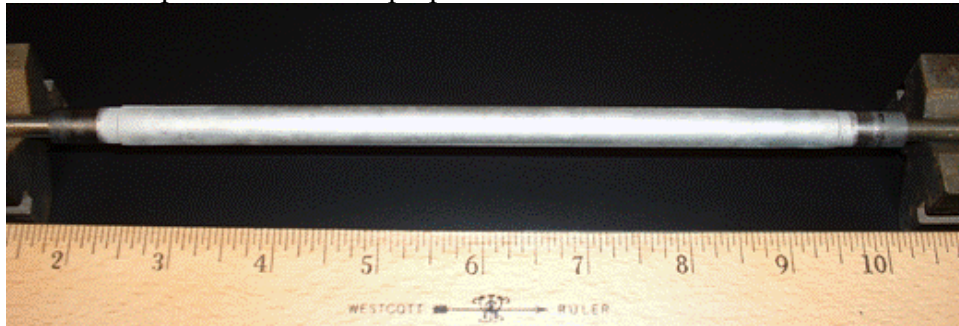


**Figure 17.** Observed hydrogen permeation rate as a function of temperature and hydrogen partial pressure differential for the 032307-2 composite membrane.

Composite membranes prepared by two versions of substrates are shown in Figure 18 below:

Composite membrane prepared with 060606 series substrate



Composite membrane prepared with 082806 series substrate

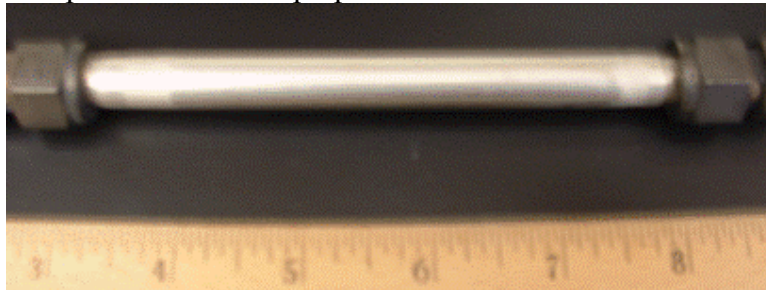


**Figure 18.** Photographs of composite membranes with short substrate tubes.

### 5.0 Task 2 – Scale-up of Composite Membrane Tubes to Longer Lengths

Based on the results obtained with short tubes in Task 1, a first-generation scale-up of the substrate tubes and composite membranes was undertaken in Task 2 with preparation of 14” long tubes with an active membrane length of 12”. Ten tubes of the series 111006 were received from Pall Corporation consisting of five tubes prepared by “B1” Zirconia coating technique and five tubes prepared with “B2” Zirconia coating technique with slightly greater coating integrity compared with “B1” coating technique. The Pd-alloy plating process was successfully scaled-up to accommodate the longer length with preparation of 10 composite membrane tubes. The results obtained with 111006-1 composite membrane, shown in Figure 19, demonstrate membrane performance similar to that shown in Figure 15 with 082806-6B membrane, thus indicating successful scale-up of the membrane. Due to high hydrogen permeate flow rate, the feed side pressure was limited to 20 psig to minimize pressure drop and cooling of the membrane tube. The observed pure component selectivity for H<sub>2</sub> permeation was about 825 compared to nitrogen at 600 °C.

The results obtained with 111006-10 composite membrane over two 25-600 °C thermal cycles, shown in Figure 20, demonstrate reproducible membrane performance and stability against thermal cycling. Due to high hydrogen permeate flow rate, the feed side pressure was limited to 20 psig to minimize pressure drop and cooling of the membrane tube. The observed pure component selectivity for H<sub>2</sub> permeation for this membrane was about 3,900 compared to nitrogen at 600 °C temperature. Three membranes prepared from this series of substrates were used in the three-tube module assembled to demonstrate WGS membrane reactor for hydrogen production in Task 3 as discussed later.

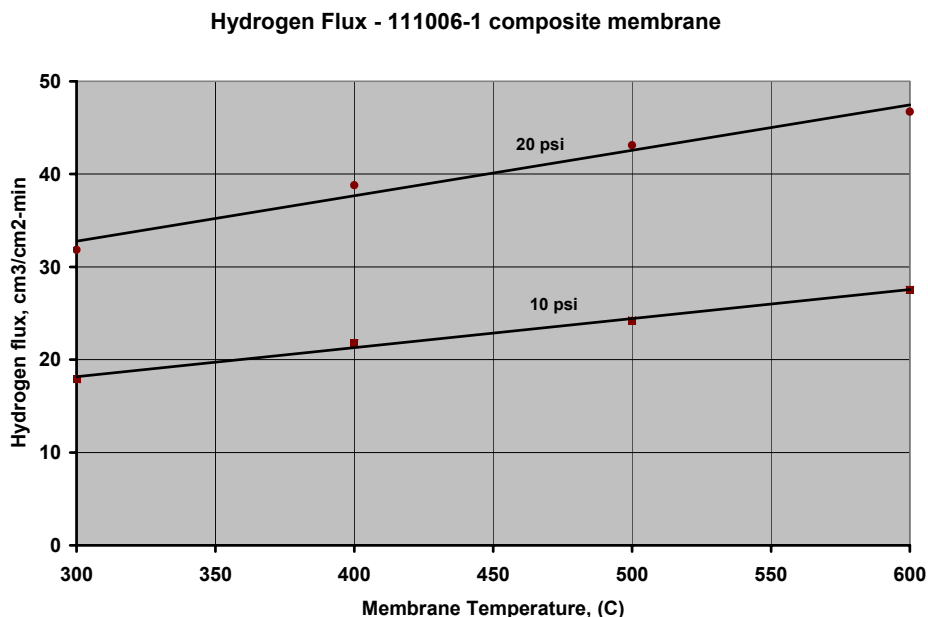


**Figure 19.** Observed hydrogen permeation rate as a function of temperature and hydrogen partial pressure differential for the 111006-1 composite membrane.

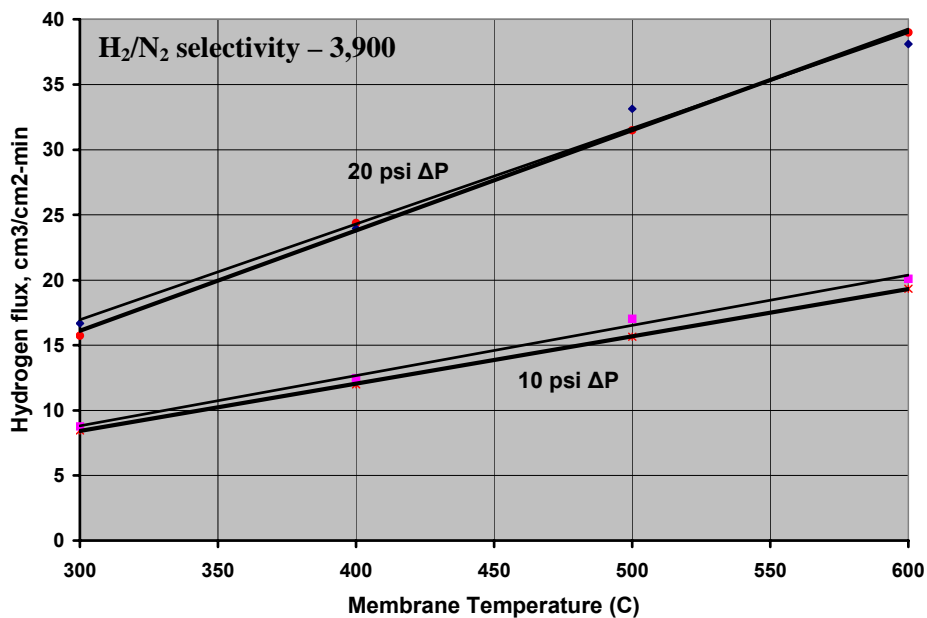


**Figure 20.** Observed hydrogen permeation rate as a function of temperature and hydrogen partial pressure differential over two thermal cycles for the 111006-10 composite membrane.

A photograph of membrane prepared with 111006 series of substrates is shown below in Figure 21.

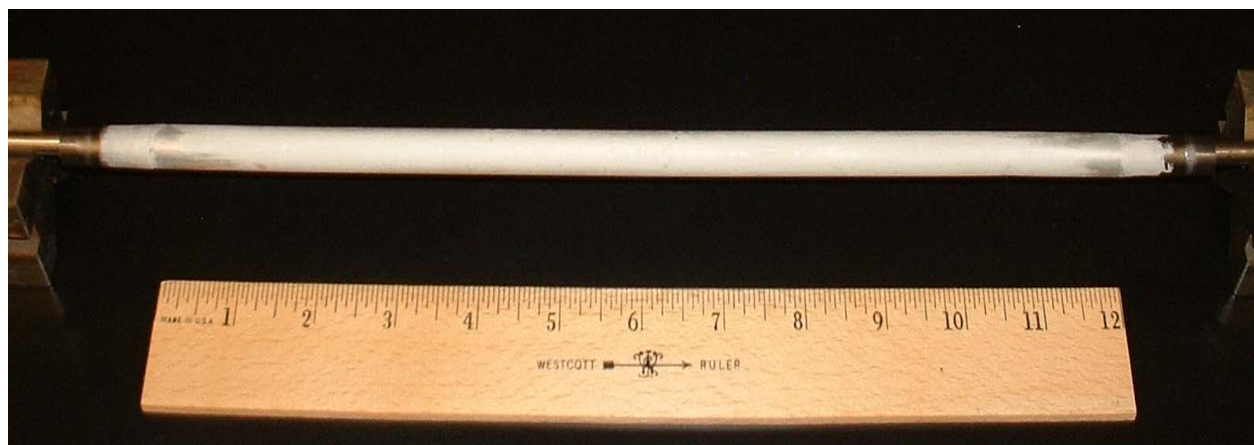


**Figure 21.** Composite Pd-alloy membrane prepared with 12” active membrane length.

A second generation (052907 series) of scaled-up substrate tubes using modified substrate formulation were supplied by Pall Corporation with an overall length of 14” and an active membrane length of 12”. A batch of ten (10) tubes of series 052907 was received by RTI to prepare and test composite membranes. Pd-Ag alloy composite membranes were prepared with these substrates using a modified plating process designed to obtain thinner membranes with much shorter plating time and were tested for their permeation characteristics. Figure 22 shows hydrogen permeation characteristics for the Pd-Ag alloy composite membrane tube 052907-11.

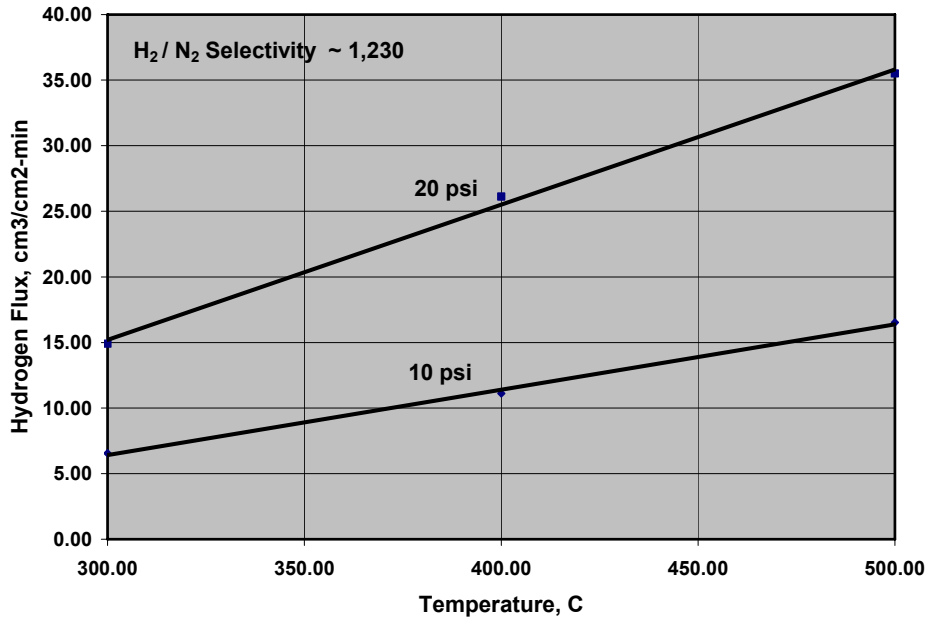


**Figure 22.** Observed hydrogen permeation rate as a function of temperature and hydrogen partial pressure differential for the 12” long 052907-11 composite membrane.

A third generation of the scaled-up 12” long substrate tubes was received from Pall Corporation nearly at the end of this project with improved quality and uniformity of the zirconia coating leading to greater bubble point pressure for liquid breakthrough. The porous metal support material was changed from 316L to 310SC stainless steel, the support tube was made slightly denser than the earlier 316L tube to better withstand the target hydrocarbon reforming gas environment. The 310SC alloy has better strength at elevated temperatures as well as better resistance to oxidation compared to 316L. The higher density was also introduced to help achieve greater strength. The nonporous end fitting welded to the porous tube was changed from a 3/8" diameter to a 10 mm diameter so that the wall thickness would be greater where the fitting is applied. The material of the end fitting was also changed from 316L to 310SC. The observed hydrogen flux rates with 977-Z3 composite membrane tube from the latest generation of the 12” substrate tubes are shown in Figure 23 and were similar to the earlier results since the average pore size of the zirconia layer remained the same leading to similar film thicknesses.

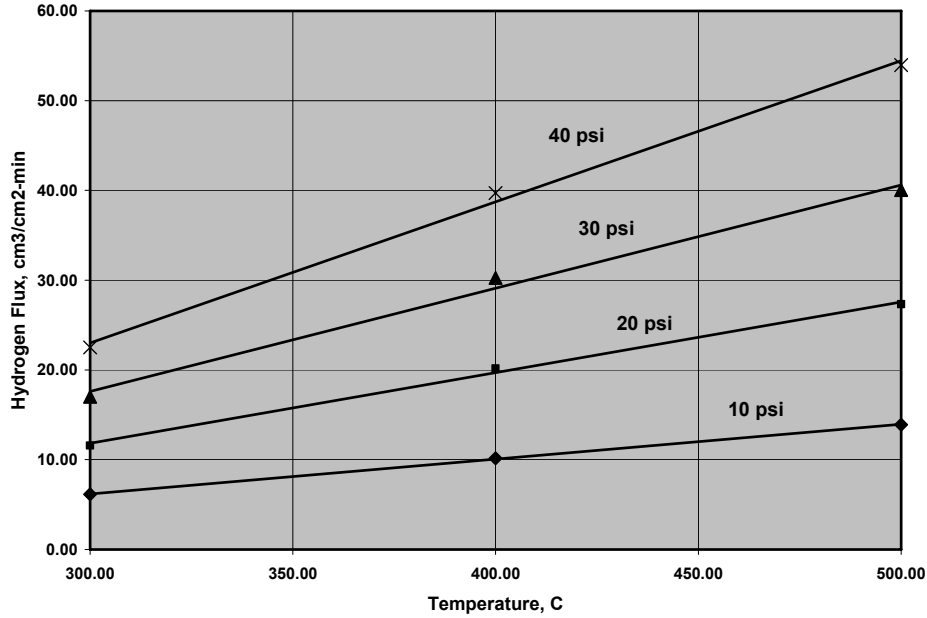


**Figure 23.** Observed hydrogen permeation rate as a function of temperature and hydrogen partial pressure differential for the 12” long 977-Z3 composite membrane element.

**6.0 Task 3 – Membrane Module Preparation and Testing**

The objective of this task was to prepare and demonstrate a pilot-scale membrane module capable of producing and separating a target 7 kg/day of hydrogen (~54 std. liters/min) using membrane elements prepared with optimized synthesis parameters and specifications. A skid-mounted pilot-scale membrane module test system was assembled capable of membrane testing at up to 300 psig and 600 °C. A three-tube membrane module with a total membrane area of 300 cm<sup>2</sup> was used to demonstrate simultaneous water gas shift (WGS) reaction and hydrogen separation for producing high purity hydrogen. A six-tube membrane module with a total membrane area of 600 cm<sup>2</sup> was assembled for demonstrating one-step steam methane reforming with simultaneous hydrogen separation for high-purity hydrogen production.

Prior to conducting the WGS reaction test with a multi-tubular membrane module in the pilot-scale system, the concept of membrane reactor operation was demonstrated in the test apparatus used for determining hydrogen permeation characteristics of single membrane tubes. The single-tube membrane test apparatus was modified for WGS reaction experiments by packing high temperature WGS catalyst (commercially available C12-Süd-Chemie Fe-Cr catalyst) around the membrane tube on the shell side (feed gas side). Separation of product hydrogen from the feed side reaction mixture is predicted to significantly increase the conversion of carbon monoxide present in the feed gas. A premixed reformat gas mixture simulating the composition of the synthesis gas generated by steam reforming of methane at commercial conditions of 900 °C and steam-to-methane ratio of 3 was used as feed gas in the single-tube as well as the multi-tubular pilot-scale WGS membrane reactor experiments. The reformat gas mixture consisted of 75.2% H<sub>2</sub>, 15.6% CO, 7.1% CO<sub>2</sub>, and 2.1% CH<sub>4</sub>. The single-membrane-tube WGS experiments were conducted using the 082806-8B

membrane tube tested earlier (active membrane area  $\sim 31 \text{ cm}^2$ ) with feed gas flow rate, feed gas pressure, and membrane temperature as test parameters. Desired steam flow rate was generated by controlling water injection flow rate using a high-pressure water pump and evaporating water in the furnace before mixing with the inlet feed gas. Steam flow rate was controlled to achieve a steam-to-CO ratio of 1.2 in the feed gas for all of the WGS experiments. The single-tube membrane reactor experiments were conducted both with and without the catalyst to determine the effect of hydrogen separation on reaction conversion.

The theoretical increase in CO conversion in the WGS reaction as a result of simultaneous hydrogen separation was predicted by a simple, one-dimensional model<sup>14</sup> of the membrane reactor concept shown schematically in Figure 24. The basic assumptions of this simple model are: 1) temperature and total pressure are constant on both permeate and feed sides; 2) reaction kinetics is faster than the hydrogen permeation flux rates, allowing the feed side to be in a dynamic equilibrium; and 3) hydrogen flux is determined by the local driving force. Model simulations were conducted to predict CO conversion and hydrogen recovery in the WGS membrane reactor at the experimental conditions studied.

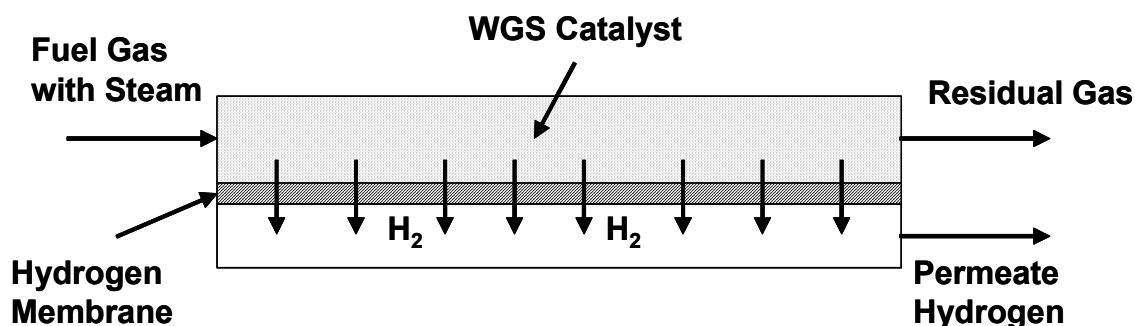


**Figure 24.** Schematic of a one-dimensional membrane reactor model.

The observed CO conversions in the single-membrane-tube experiments are compared with the theoretical model predictions in Figure 25. The model predictions assume fast WGS kinetics and dynamic feed side equilibrium along the length of the membrane as hydrogen is permeated. The experiments clearly demonstrated the effect of hydrogen separation on increasing CO conversion. At 450 °C membrane reactor temperature, the effect of WGS reaction kinetics was also significant, as seen by the effectiveness of catalyst on increasing CO conversion. At a membrane operating temperature of 550 °C, however, the WGS reaction rate was found to be much faster even without any catalyst, as indicated by the observed CO conversion approaching the model prediction in Figure 26.

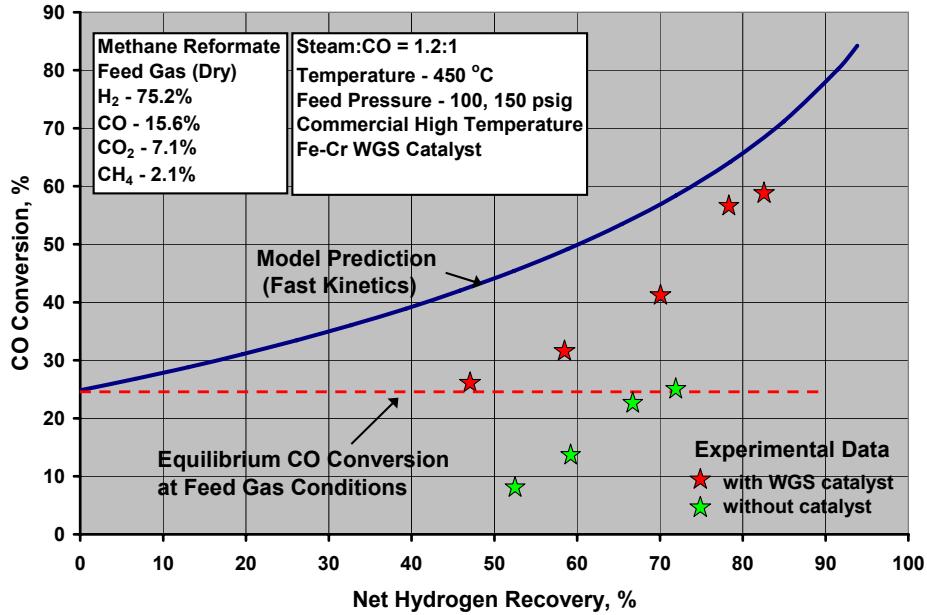


**Figure 25:** Observed CO conversion in membrane reactor experiments with and without catalyst.

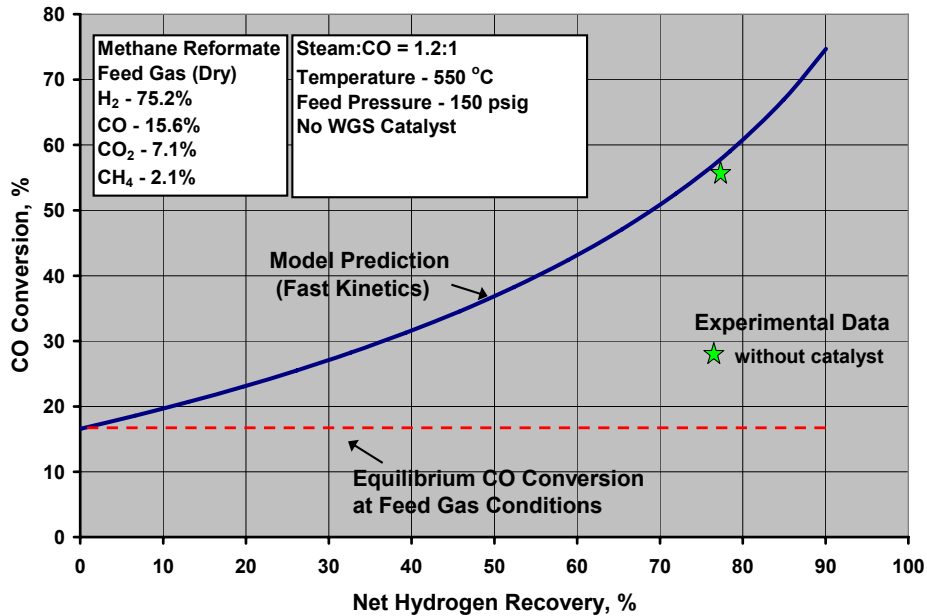


**Figure 26:** Observed CO conversion in membrane reactor experiments without catalyst at 550 °C.

A pilot-scale, skid-mounted membrane test system was assembled using a multi-tubular module with an online data acquisition and control system. A membrane module is housed in a tubular stainless steel shell 2.5” ID and 42” length designed to accommodate up to 30” long membrane tubes for membrane testing up to 300 psig feed pressure and up to 600 °C membrane temperature. The furnace, with an ID of 4” and a three-zone heater of 36” in length, is able to accommodate up to 3.5” OD membrane housing shell. The membrane tubes are operated in a dead-end configuration. The feed gas is introduced at the bottom of the housing and flows on the shell side of the membrane

module. The permeate gas from each tube is collected in a manifold in the bottom flange. Although no flow through sweep gas is used for the membrane tubes, the permeate side of the membrane module may be flushed with an inert gas by pressurizing/depressurizing the permeate side space and then maintaining a small inert gas flow in the manifold. Desired steam rate is generated by controlling water flow rate using a high pressure water pump and evaporating water in the furnace before mixing with the inlet feed gas stream. The inlet feed gas is preheated before mixing with steam. The lower flanges of the shell are heated by band heaters and all of the inlet gas lines are heat-traced for preventing any water condensation. Both the exit feed gas and permeate are cooled in water-cooled condensers to separate water vapor if present. The feed gas flow is controlled by a mass flow controller. The feed and permeate pressures are regulated by back-pressure regulators. The exit feed gas flow rate and permeate flow rate are monitored by respective mass flow monitors. Both the exit feed gas and the permeate gas streams may be sampled by a gas chromatograph for real-time analysis of gas streams during experiments. A LabView-based monitoring and control system by National Instruments is used to monitor process temperatures, pressures, and flow rates and for controlling temperature of each of the three heating zones in the furnace. Figure 27 shows a picture of the pilot-scale system.



**Figure 27:** Photograph of the pilot-scale test skid. The picture also shows a three-membrane tube module housed inside a 36"-long three-zone furnace.

A three-tube membrane module was used for the pilot-scale WGS membrane reactor experiments. The membrane module held three membrane elements between two support rings (Figure 28). The lower ring with small perforated openings provided support for WGS catalyst loaded around the tubes in the membrane housing shell. The upper ring with much wider openings allowed loading of

the catalyst in the shell. Each of the membrane tube was capped on the top with the lower ends connected to the permeate manifold in the bottom flange to withdraw permeated hydrogen. The 3-tube module with membrane elements of 12" active length provided a total membrane area of 300 cm<sup>2</sup>. The membranes used in the WGS experiments were prepared using the substrates from the 111006 series. The same housing module will also be able to house the anticipated commercial size 30" active membrane length elements with a total membrane area of 750 cm<sup>2</sup>. The system furnace itself will be able to accommodate up to 3.5" ID shell.



**Figure 28.** Three-tube membrane module held between two rings and Swagelok fittings.

The three-tube module used for WGS membrane reactor experiments along with the module housing shell (2.5" ID and 42" length,) and the operating pilot skid system with a dedicated gas chromatograph for real-time analysis of various gas streams and a computer-controlled reactor monitoring and control system is shown in Figures 29, 30, and 31, respectively.



**Figure 29.** Housing shell for multi-tubular module, 2.5" ID, 42" length.

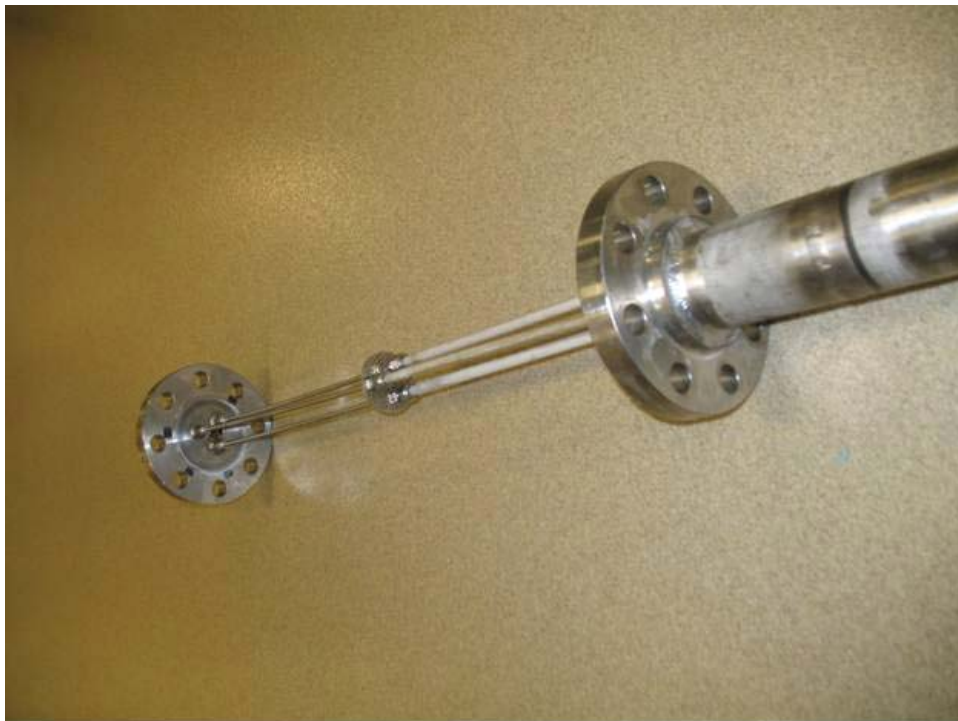


**Figure 30.** Membrane module being loaded iton the housing shell.



**Figure 31.** Functional pilot-scale skid with GC and computer control system.

WGS membrane reactor experiments were conducted with the three-tube membrane module using a simulated natural gas reformat composition as a feed gas. The premixed reformat gas mixture simulated the composition of the synthesis gas generated by steam reforming of methane at commercial conditions of 900 °C and steam-to-methane ratio of 3 and consisted of 75.2% H<sub>2</sub>, 15.6% CO, 7.1% CO<sub>2</sub>, and 2.1% CH<sub>4</sub>. Steam was introduced along with the feed reformat gas to provide a steam-to-CO ratio of 1.2 in all of the WGS membrane reactor experiments. High-temperature WGS catalyst (commercial Fe-Cr based catalyst - Shiftmax 120 provided by Süd-Chemie, Inc.) was used in these experiments.

The WGS membrane reactor experiment operating conditions included 100 and 150 psig feed pressure, 375 and 550 °C membrane reactor temperature, and various feed gas flow rates to allow varying the net hydrogen recovery for a given experiment. More than 80% conversion of CO and product hydrogen recoveries greater than 80% of the maximum possible hydrogen potential were demonstrated as shown in Figure 32. Also as seen in Figure 32, the equilibrium CO conversion for the feed gas composition used, membrane reactor temperature of 375 °C, and steam-to-CO ratio of 1.2 was about 45%. However, CO conversion much greater than the equilibrium conversion was demonstrated in these experiments by continuous removal of product hydrogen from the reaction mixture. Even at a higher reaction temperature of 550 °C with an unfavorable equilibrium conversion of CO of only 17%, much greater CO conversions than the equilibrium conversion are seen in Figure 33 due to simultaneous hydrogen separation in the membrane reactor module. The observed hydrogen purity was 98.5% for operation at 100 psig pressure and 97.5% for operation at 150 psig pressure.

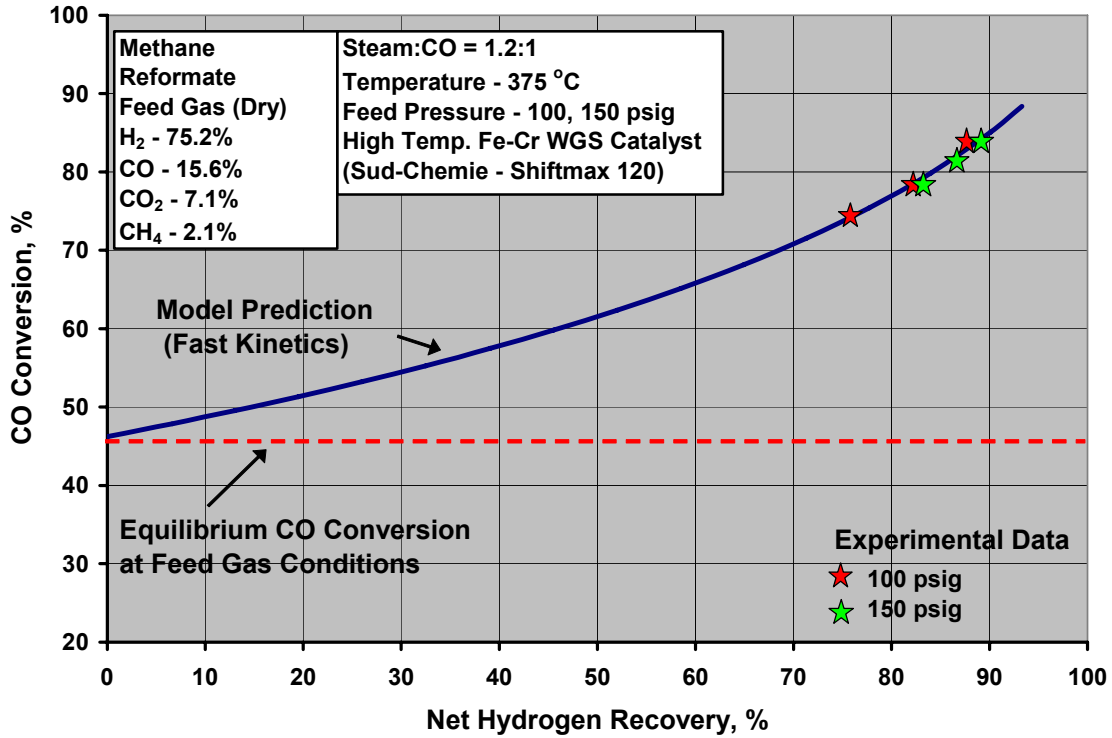


Figure 32. Observed CO conversion as a function of net hydrogen recovery at 375 °C.

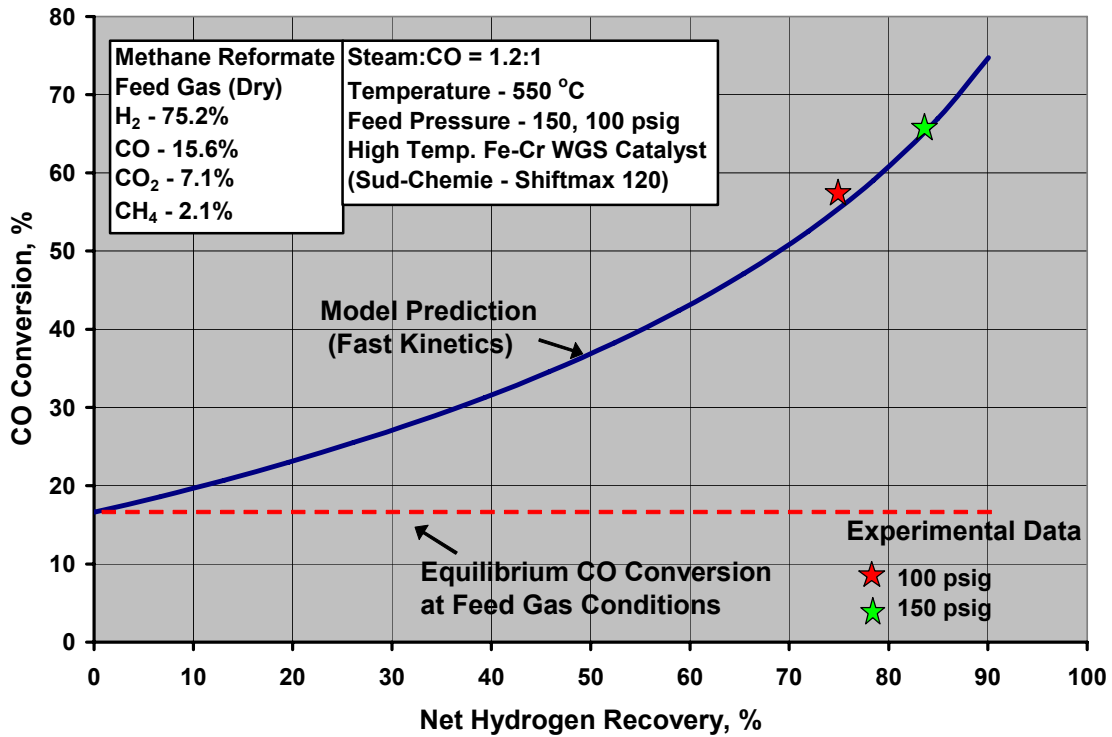
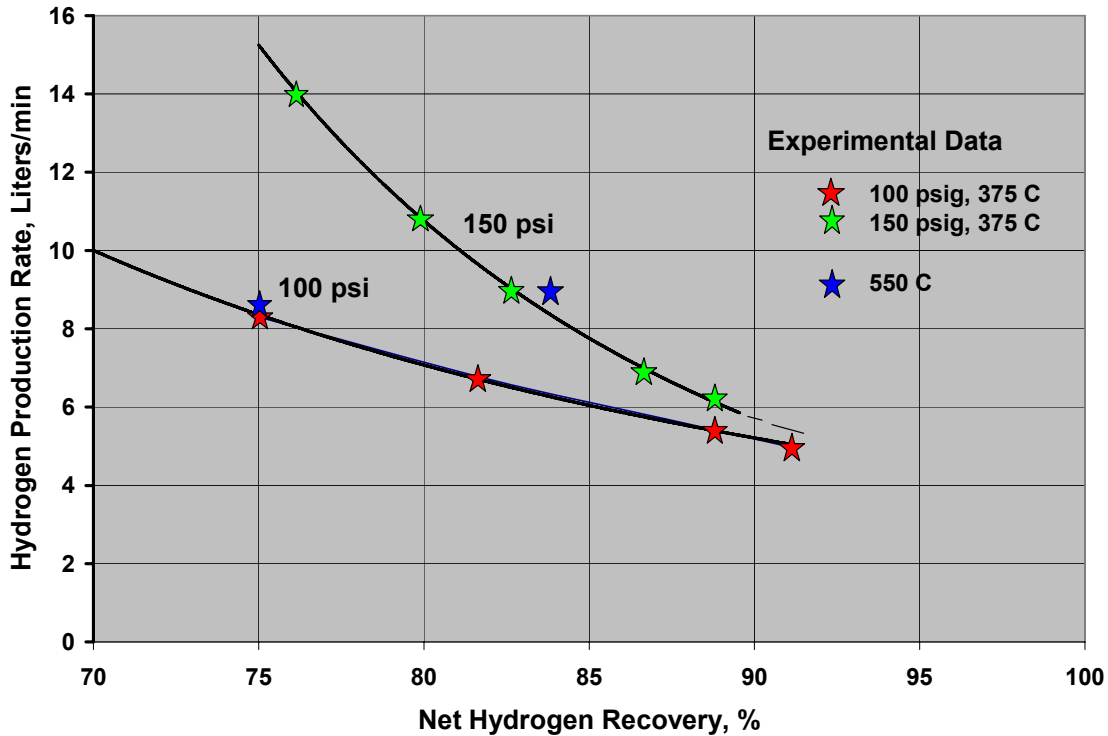


Figure 33. Observed CO conversion as a function of net hydrogen recovery at 550 °C.

The amount of hydrogen that can be produced by the membrane reactor strongly depends on the feed side pressure and the net hydrogen recovery. As seen in Figure 34, hydrogen productivity decreases with increasing net hydrogen recovery due to lower hydrogen driving force becoming available as hydrogen recovery is increased. By increasing the feed side pressure while keeping the permeate pressure constant at ambient pressure increases hydrogen productivity of the module significantly. Although a higher membrane temperature allows greater hydrogen permeation rate, the greater hydrogen permeability of the membrane was offset in these experiments due to increased observed methane formation at the higher temperature of 550 °C which consumes hydrogen and reduces the hydrogen partial pressure on the feed side reducing the hydrogen driving force for permeation. As a result, hydrogen productivity was not affected significantly by operating the membrane module at a higher temperature of 550 °C when compared to that observed at 375 °C at the same feed side pressures. At the targeted operation of the membrane module at 300 psig feed side pressure and 80% net hydrogen recovery, about 20 liters/min hydrogen production is anticipated with the 300-cm<sup>2</sup> membrane area module. With the scaled-up elements with 30” active length, a three-tube module is projected to produce 50 liters/min of hydrogen, the target for this pilot-scale skid system.



**Figure 34.** Hydrogen productivity of the three-tube module.

In addition to conducting the WGS reaction in a membrane reactor, it would also be possible to conduct steam methane reforming in a single step in the membrane reactor configuration at much milder reaction conditions of 600 °C than that used in a conventional process. Model simulations indicated that greater than 90% conversion with greater than 90% recovery of maximum possible hydrogen is theoretically possible as seen in Figure 35.

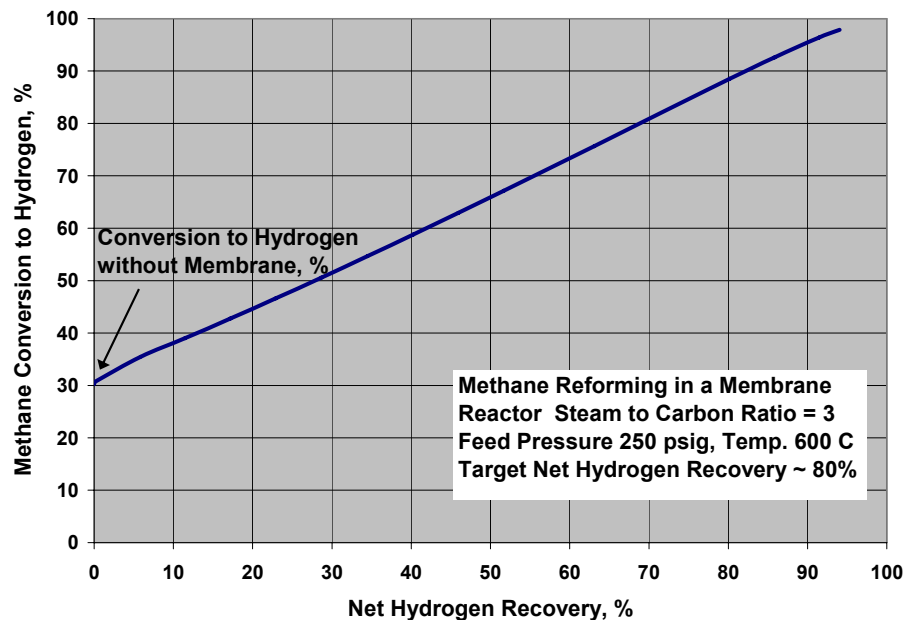


**Figure 35.** Predicted increase in methane conversion in a membrane reactor.

Six composite membranes prepared using the last series of the scaled-up substrate tubes was assembled in a module along with methane reforming and WGS catalysts, as shown in Figure 36.

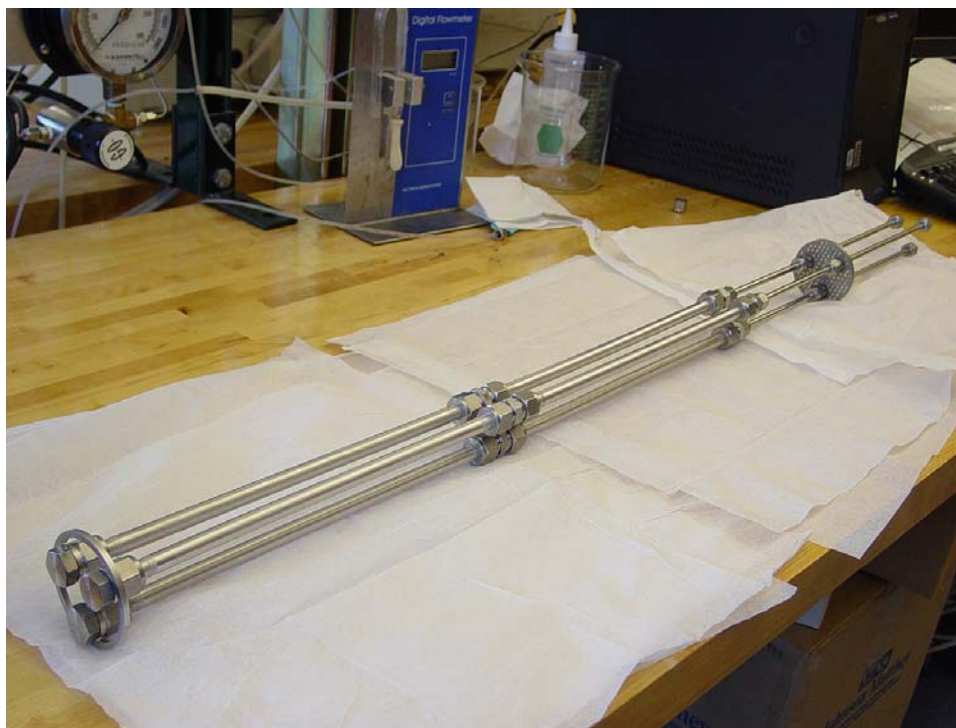


**Figure 36.** Six-tube membrane module assembled for the methane reforming demonstration.

As seen from the picture (Figure 36) the membrane module allowed loading of the methane reforming catalyst (commercial FCR-70 Nickel-based catalyst provided by Süd-Chemie) in a short 6” section before the membranes for partial reforming of methane by steam prior to beginning hydrogen separation. The membrane tube sections were packed with both the methane reforming catalyst (FCR-70) and WGS reaction catalyst (C-12) provided by Süd-Chemie. Figure 37 shows the membrane module loaded in the housing shell with the permeate tubes connected to the permeate manifold in the bottom flange of the shell. This configuration allows production of high-purity hydrogen from methane.



**Figure 37.** Six-membrane module connected to the permeate manifold in the bottom flange.

#### **7.0 Task 4 – Technical and Economic Evaluation and Commercialization**

Palladium-alloy based membranes have been known to be completely selective for hydrogen permeation and are used in commercially available small scale hydrogen purification units<sup>15,16,17</sup>. These hydrogen purification units typically use palladium-alloy foils 25-30 microns thick or tubes (60-100 microns thick) to produce high-purity hydrogen (e.g., 99.99999%) for specialized applications using industrial-grade hydrogen. The small-scale hydrogen purifiers are expensive on unit hydrogen flow basis. Since membrane systems are modular in nature (i.e., larger capacities are provided by adding more modules or increasing membrane surface area linearly), palladium foil or tube-based hydrogen separation is likely to be cost-prohibitive for large-scale hydrogen separation applications. Palladium alloy foils or tubes have also been incorporated in small hydrocarbon fuel reformers that are being demonstrated<sup>18,19,20</sup> for producing hydrogen. Palladium alloy membranes are used either to purify the product hydrogen after a fuel reformer<sup>18,19</sup> or integrated within the fuel

reforming process<sup>20</sup>. The hydrogen capacity of such available units is designed to support a PEM fuel cell power rating of a few kW or <100 std. liters of H<sub>2</sub>/min or less.

The cost of Pd-alloy membranes used for hydrogen separation may be reduced by depositing a thin Pd-alloy film on a suitable porous substrate to form a composite membrane, as pursued in this project. Low-cost Pd-alloy composite membranes will be attractive for both hydrogen separation applications or for hydrogen production by membrane reactor applications. Pd-alloy membranes are, however, most likely to be commercially viable for applications where they can make significant impact on both the capital cost of the system as well as on the overall cost of product hydrogen. For large-scale hydrogen facilities such as centralized hydrogen production, the capital cost of the production plant is responsible for only about 20% of the product cost, so maximizing process efficiency drives reactor design. For smaller hydrogen production facilities, the capital cost is much more important, so minimizing capital cost dictates reactor design. The Pd-alloy membrane reactor makes it possible to combine two unit operations, reaction and purification, into one unit; hence, by reducing the number of pieces of equipment, it is possible to reduce capital cost of the hydrogen production system. Pd-alloy based hydrogen production process is therefore likely to be commercially viable for small- to mid-range hydrogen production facilities such as those envisioned for distributed hydrogen production at hydrogen refueling stations and for distributed power generation facilities based on PEM fuel cells.

Currently, over 80% of hydrogen is produced by steam reforming of natural gas followed by hydrogen separation as being the most economical option, depending upon availability of natural gas<sup>21</sup>. Hydrogen will ultimately need to be produced totally from renewable energy sources for sustainable hydrogen economy; however, for the near-term transition period, hydrogen will need to be produced from fossil fuels, primarily natural gas and coal. The industry standard process for hydrogen production from natural gas involves natural gas reforming producing synthesis gas, followed by two-stage WGS reactor and hydrogen purification by Pressure Swing Adsorption (PSA). As shown in Figure 38, the Pd-alloy based membrane reactor technology will combine the WGS reactor and PSA in a single unit. Further system integration may also be possible by combining natural gas reforming and WGS reactions with hydrogen purification in one unit.

The most important performance metric is the capital cost per unit amount of hydrogen produced. The U. S. Department of Energy has established year 2010 target of 250 scfh/ft<sup>2</sup> for hydrogen flux with an installed module cost target of \$1,000/ft<sup>2</sup>.<sup>9</sup> Assuming a conservative Pd-alloy membrane thickness of 4 μm, the cost of the expensive Pd/Ag alloy metal in the membrane is estimated to be ~\$54/ft<sup>2</sup> (June 2008 prices). Considering the cost of substrate materials to be about \$100/ft<sup>2</sup>, the DOE cost goal of \$1,000/ft<sup>2</sup> would be quite achievable. From a commercial perspective, these goals are both flexible and dependent on each other. For example, if the flux could be doubled, it could be permissible to increase the cost. Likewise, a lower flux would be acceptable at a lower cost. Combining these goals into a final goal of \$4/scfh of hydrogen capacity sets a relevant, challenging goal for commercialization.

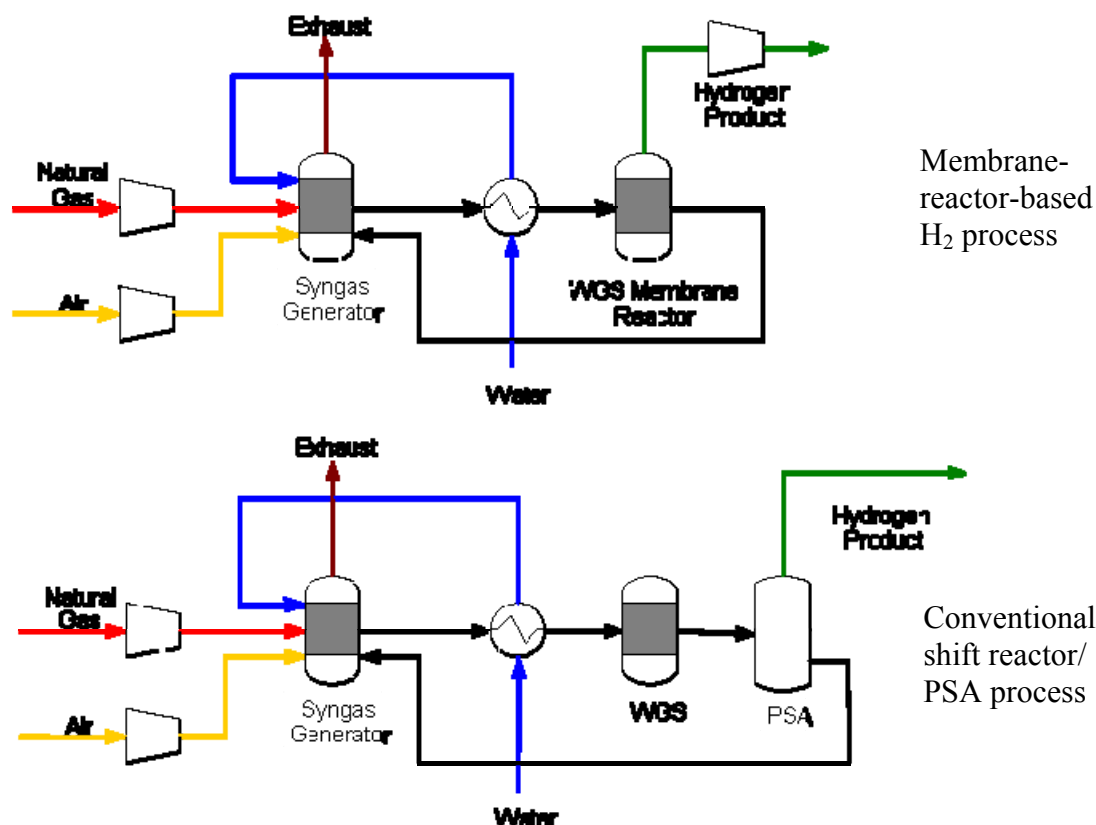


**Figure 38.** Conventional and membrane-reactor-based hydrogen processes.

U. S. DOE has developed a hydrogen production cost analysis model<sup>22</sup> which may be used to determine potential for membrane reactor technology for reducing cost of hydrogen production. For the base case hydrogen production of 100 kg/day (1650 scfh or about 40 MW equivalent), the experimental data obtained with the developmental Pd-alloy composite membranes in this project indicate that about 15 ft<sup>2</sup> of membrane area would be needed. Assuming U. S. DOE's membrane module cost target is met, the cost of WGS membrane reactor module for 100 kg/day hydrogen plant would be about \$15,000. (The cost of Pd/Ag alloy metal in the module is estimated to be \$810.) For the same hydrogen capacity, the cost of conventional WGS reactor/PSA system is estimated to be about \$55,000 with a potential cost reduction by the membrane reactor system of \$40,000. The capital cost portion for the baseline case of 100 kg/day hydrogen plant is estimated to be about \$3.06/kg of hydrogen by the H<sub>2</sub>A forecourt model. Reducing the plant capital cost by \$40,000 is predicted to reduce the cost of hydrogen production by \$0.36/kg of hydrogen according to the forecourt cost model. The membrane reactor process produces hydrogen at a lower pressure. If the hydrogen produced could be used at a lower pressure (e.g., by a PEM fuel cell for power generation), all of the predicted cost reduction could be realized. However, if hydrogen compression is required, the membrane reactor process will incur additional cost for compressing hydrogen from ambient pressure to 300 psig assumed for the conventional PSA-based process. Assuming 50% increase in the compressor capital cost for the additional compression needed, the impact on the cost of hydrogen production would be about \$0.08/kg of hydrogen, thus reducing potential cost benefit of

the membrane reactor process to about \$0.28/kg of hydrogen. The potential cost benefits are expected to be greater for hydrogen production plants smaller than the base case of 100kg/day (~40 MW) considered here. For a residential power generation unit, a capacity of 5 kW is considered to be adequate, whereas, for distributed power generation applications, capacities of 150 kW to 1 MW are considered to be typical. The Pd-alloy based hydrogen process would thus be attractive for the residential or distributed power generation market as well.

Above preliminary analysis indicates that membrane reactor process has potential to reduce the cost of hydrogen production, especially for small-scale systems. Additional benefits of the membrane reactor approach not considered/quantified in this analysis include increased hydrogen yield per unit of fuel feedstock used and reduced energy and operational cost due to simpler membrane reactor operation compared to a PSA system.

## 8.0 Conclusions:

- Substantial progress was made in improving the quality of the palladium-alloy composite membranes prepared by depositing thin Pd-alloy films by electroless plating technique on tubular inorganic porous substrate materials consisting of ceramic Zirconia coating on porous stainless steel tubes. Improvements in substrate material and composite membrane are still ongoing.
- Improvements in substrate materials included procedures for depositing Zirconia layer, integrity and thickness of the zirconia layer, welding nonporous ends, Zirconia surface treatment/smoothing, changing grade and porosity of the base porous stainless steel material, changing size of porous tube as well as non-porous end tubes, and developing a process for suitable for mass manufacturing.
- Improvements in composite membrane preparation technique included changing plating times and sequencing to change membrane thickness according to the quality of substrate materials, elimination of intermediate drying steps, and continuous sequential plating of different metals necessary for mass production.
- Hydrogen to nitrogen selectivity greater than 1,000 was consistently observed in permeation tests of different versions of substrate materials. The hydrogen flux of the composite membranes at 400 °C and 20 psi transmembrane pressure differential was typically in the range of 20-40 cm<sup>3</sup>/cm<sup>2</sup>·min, lower than U.S. DOE hydrogen flux target by a factor of 3-4.
- Substrate materials and composite membranes were successfully scaled up to 12” active membrane length with membrane area of 300 cm<sup>2</sup>.
- More than 80% CO conversion and product hydrogen recoveries greater than 80% of the maximum possible hydrogen potential were demonstrated in WGS membrane reactor experiments conducted with a three-tube membrane reactor module.
- A functional, pilot-scale hydrogen separation module was developed to produce high-purity hydrogen directly from methane.
- Preliminary techno-economic analysis conducted with DOE’s H2A model indicated that Pd-alloy membrane reactor-based hydrogen process has potential to reduce the cost of hydrogen production, especially for small-scale systems, and would be attractive for distributed hydrogen production or for residential or distributed power generation.

## 9.0 References:

1. U. Balachandran, "Development of Dense Ceramic Membranes for Hydrogen Separation," Proceedings of 2005 U.S. DOE Hydrogen Annual Merit Review Meeting, Arlington, VA, May 2005.
2. M. Schwartz, S. Gade, R. Schaller, and B. Berland, "Novel Composite Membranes for Hydrogen Separation in Gasification Processes in Vision 21 Plants," Presented at the 19<sup>th</sup> Annual International Pittsburgh Coal Conference, Pittsburgh, PA, September 2002.
3. B. L. Bischoff and R. R. Judkins, "Scale-Up of Microporous Inorganic Hydrogen-Separation Membranes," Proceedings of 2006 U.S. DOE Hydrogen Annual Merit Review Meeting, Arlington, VA, May 2006.
4. A. S. Damle, G. N. Krishnan, A. Sanjurjo, B.J. Wood and K.H. Lau, "Thermal and Chemical Degradation of Inorganic Membrane Materials," Final Report, DOE Contract DE-AC21-92MC28053, May 1995.
5. S. Uemiya, T. Matsuda and E. Kikuchi, "Hydrogen permeable palladium-silver alloy membrane supported on porous ceramics," *J. Membrane Sci.*, **56**, 315 (1991).
6. F. Roa, J.D. Way, R.L. McCormick, and S.N. Paglieri, "Preparation and Characterization of Pd-Cu Composite Membranes for Hydrogen Separation," *Chem. Eng. J.*, 93, No.1 pp 11-22, 2003.
7. I. P. Mardilovich, E. Engwall and Y.H. Ma, "Dependence of hydrogen flux on the pore size and plating surface topology of asymmetric Pd-porous stainless steel membranes", *Desalination*, **144**, 85-89 (2002).
8. A. S. Damle, "Separation of Hydrogen and Carbon Dioxide in Advanced Fossil Energy Conversion Processes using a Membrane Reactor," Proceedings of the 2002 Pittsburgh Coal Conference, Pittsburgh, September 2002.
9. U. S. Department of Energy, Washington, D.C, Multi-Year Research, Development and Demonstration Plan, Page 3.1-17, accessed June 2008 at <http://www1.eere.energy.gov/hydrogenandfuelcells/mypp/pdfs/production.pdf>
10. A. J. Burggraaf and K. Keizer, "Synthesis of Inorganic Membranes," in *Inorganic Membranes Synthesis, Characteristics, and Applications*, R. Bhavé Editor, p. 10, Van Nostrand Reinhold, New York, (1991).
11. A. S. Damle, "Method for preparation of thermally and mechanically stable metal/porous substrate composite membrane", U.S. Patent 6,761,929 (2004).
12. J. Shu, B.P.A. Grandjean, E. Ghali, and S. Kaliaguine, "Simultaneous Deposition of Pd and Ag on Porous Stainless Steel by Electroless Plating," *J. Membrane Science.*, **77**: 185-195, 1993.
13. S. Uemiya, N. Sato, H. Ando, Y. Kude, T. Matsuda, and E. Kikuchi, "Separation of hydrogen through palladium thin film supported on a porous glass tube," *J. Membrane Sci.*, **56**: 303, 1991.
14. A. S. Damle, "Hydrogen Production by Reforming of Liquid Hydrocarbons in a Membrane Reactor for Portable Power Generation – Part I Model Simulations," *J. Power Sources*, **180** (2008) 516–529.
15. Johnson Matthey, Gas Purification Technology Products information available at <http://www.jmgpt.com/> accessed June, 2008.
16. REB Research, Hydrogen Purifier products information available at <http://www.rebresearch.com/catalog.html> accessed June, 2008.

17. Power + Energy, Hydrogen Separator products information available at <http://www.powerandenergy.com/products.shtml> , accessed June, 2008.
18. IdaTech, Fuel Processing Technology and ElectrGen product information available at [http://www.idatech.com/technology/fuel\\_processors.html](http://www.idatech.com/technology/fuel_processors.html) and [http://www.idatech.com/media/pdf/ElectraGen\\_XTRModule.pdf](http://www.idatech.com/media/pdf/ElectraGen_XTRModule.pdf) accessed June 2008.
19. InnovaTek, InnovaGen Fuel Processor product information available at <http://www.tekkie.com/docs/InnovaGen.pdf> accessed June 2008.
20. Intelligent Energy, Fuel Processor and hydrogen generator product information available at [http://www.intelligent-energy.com/images/uploads/compact\\_hydrogen\\_generator\\_a4.pdf](http://www.intelligent-energy.com/images/uploads/compact_hydrogen_generator_a4.pdf) accessed June 2008.
21. J.A. Ritter, and A.D. Ebner, “Separation Technology R&D Needs for Hydrogen Production in the Chemical and Petrochemical Industries,” U.S. DOE Office of Industrial Technologies Program Report, December 2005.
22. U. S. Department of Energy, Washington, D.C., DOE H2A Analysis information accessed November 2007 at [http://www.hydrogen.energy.gov/h2a\\_analysis.html](http://www.hydrogen.energy.gov/h2a_analysis.html)